

Supporting Information

for

Aqueous Recognition of Purine and Pyrimidine Bases by an Anthracene-based Macrocyclic Receptor

Danny Van Eker, Soumen K. Samanta and Anthony P. Davis*

School of Chemistry, University of Bristol, Cantock's Close, Bristol, UK, BS8 1TS

*Corresponding Author. Email: Anthony.Davis@bristol.ac.uk

Contents

Materials and General Methods	S2-S3
Fluorescence Titrations	S4-S12
¹ H NMR Binding Studies	S13-S21
Isothermal Titration Microcalorimetry (ITC)	S22-S24
Molecular Modelling	S25-S33

Materials and General Methods.

Receptor **1** was prepared as reported previously.¹ Commercially available reagents were purchased from Sigma-Aldrich, Alfa-Aesar, Fluorochem, Frontier Scientific, VWR, Acros Organics, Frontier Scientific or Carbosynth and used as purchased unless specified otherwise. ¹H NMR spectra were recorded at 298K on a Varian VNMRs 600MHz spectrometer with cryoprobe, or a Varian 500MHz spectrometer. Chemical shifts observed in NMR spectroscopic experiments are quoted in parts per million (ppm) and referenced using residual solvent peaks for ¹H, to which the instruments were externally calibrated. Fluorescence spectra were recorded using a Horiba FluoroMax-4 fluorimeter. ITC experiments were performed on a MicroCal iTC200 at 298 K.

¹H NMR Titration Experiments

Host and guest stock solutions were made up in a phosphate buffer solution (D₂O, pH 7.4, 10 mM). A solution of receptor **1**, typically 500 μM concentration, was placed in an NMR tube and receptor **1** was also added at the same concentration to the guest solution, to ensure the concentration of receptor **1** remained constant throughout the experiment. For experiments tracking the movement of various nitrogen-based protons, host and guest were instead made up in phosphate buffer solution (pH 7.4, 10 mM), in a mixture of H₂O/D₂O (9:1). Aliquots of guest solution were added to the NMR tube, the NMR tube was inverted several times to ensure thorough mixing and the ¹H NMR spectra were recorded after each addition. Association constants were determined by plotting the change in shift (ppm) of aromatic proton verses molar equivalents using the Bindfit software.^{2,3}

Fluorescence Titration Experiments

Fluorescence titration experiments were carried out at 298 K on a Horiba Fluoromax spectrofluorimeter in quartz cuvette (3 mL, 10 mm path length). Titrations with all guests were performed in phosphate buffer solution (pH 7.4, 10 mM). The pH of receptor **1** and titrant solutions were checked before use. Receptor **1** was titrated with guests. Guest additions to the receptor **1** were performed using a procedure which kept the concentration of receptor **1** constant throughout the titration. Thus, a known concentration of receptor **1** was added to a solution of guest solution to keep the concentration of receptor **1** constant. This solution was used as titrant. For each addition, the volume of titrant was added, the cuvette was stirred for 30 second and then left to settle for a further 30 seconds before the fluorescence spectrum was recorded. The excitation wavelength was fixed at 395 nm for each titration, and the emission

spectrum recorded between 400 – 700 nm. Association constants were calculated by plotting the fluorescence intensity change versus the molar equivalent ratio between host and guest.

Isothermal Titration Microcalorimetry (ITC) Experiments.

Isothermal titration microcalorimetry (ITC) experiments were performed on a MicroCal iTC200 microcalorimeter. ITC experiments were carried out at 298 K. Guest solutions were prepared in HPLC-grade water with 10 mM phosphate buffer solution (pH 7.4) and allowed to equilibrate overnight. The sample cell was charged with a known concentration of receptor **1** solution (0.2 mL) in HPLC-grade water with 10 mM phosphate buffer solution at pH 7.4. Then, aliquots (typically 2.0 μ L for the MicroCal iTC200) of guest solution were added and the evolution of heat was followed as a function of time. Heats of dilution were measured by injecting the same guest solution into HPLC-grade water with 10 mM phosphate buffer solution at pH 7.4, using identical conditions. For every addition, the heat of dilution was subtracted from the heat of binding using MicroCal software (MicroCal iTC200 Analysis Add-On Software Package (v 7.20) for ORIGIN 7.0). This gave an XY matrix of heat vs. total guest concentration. This matrix was then imported into a specially written Excel programme to fit the data to a 1:1 binding model to give a K_a . ΔG can be derived from K_a and thus ΔS can be derived from ΔH and ΔG using common thermodynamic equations.

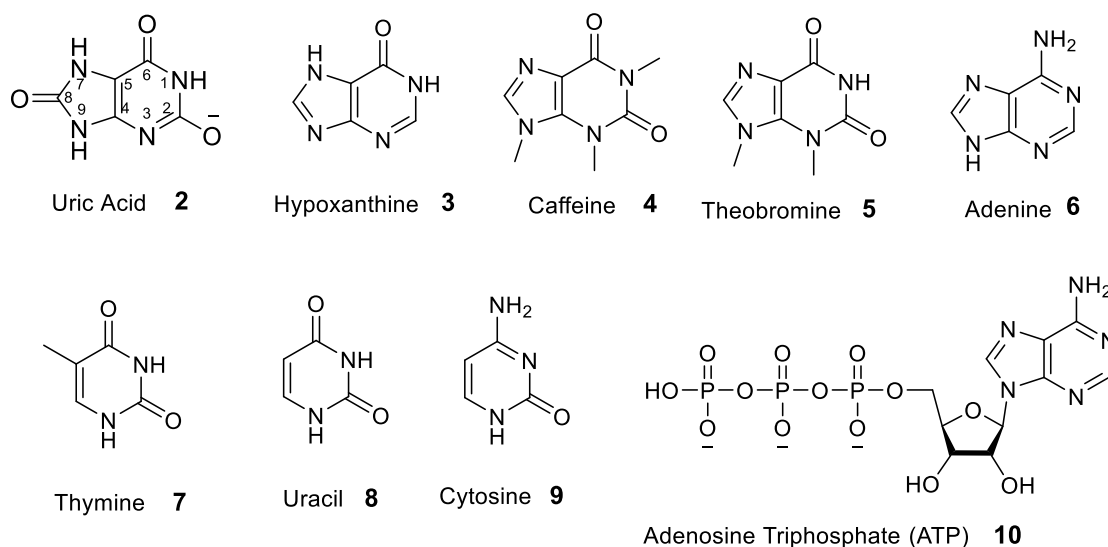


Figure S1. Chemical structure of the guests used in binding studies to receptor **1**. Uric acid **2** is represented as the monoanion.

Fluorescence Titrations

Uric acid

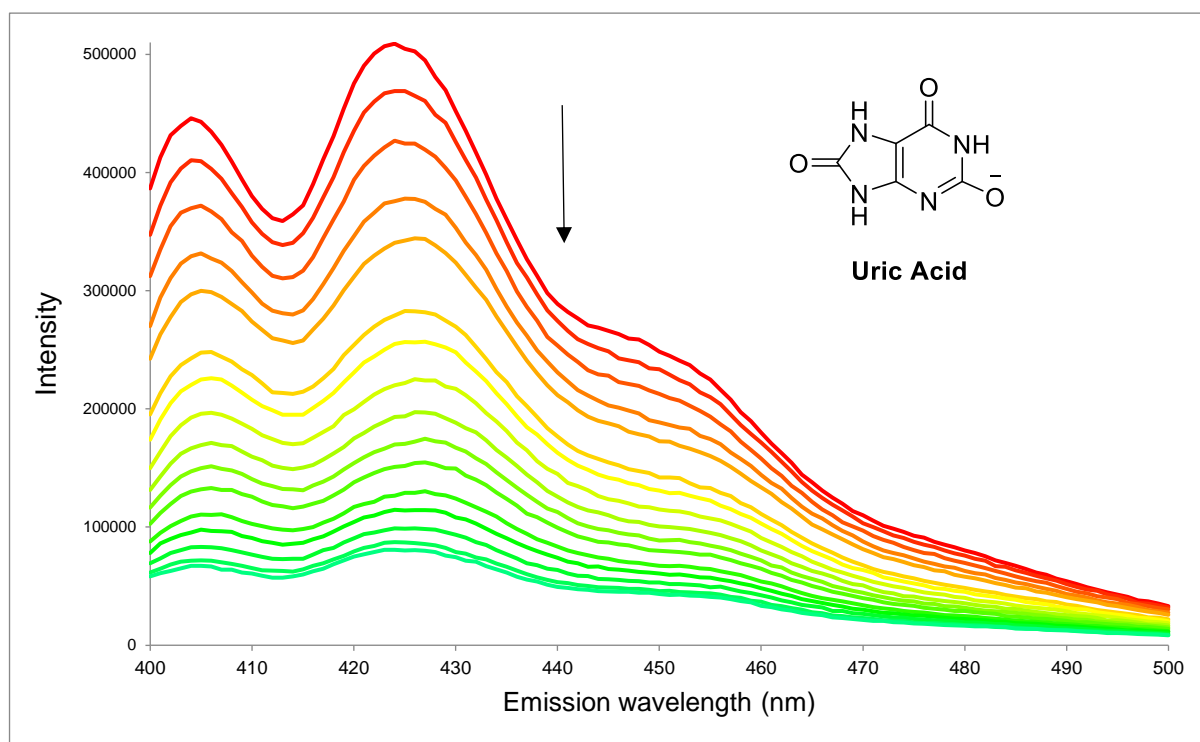


Figure S2. Fluorescence titration of receptor **1** (11.8 μM) with uric acid **2** in H₂O (pH 7.4, 10 mM phosphate buffer) at 298 K. Excitation wavelength 395 nm.

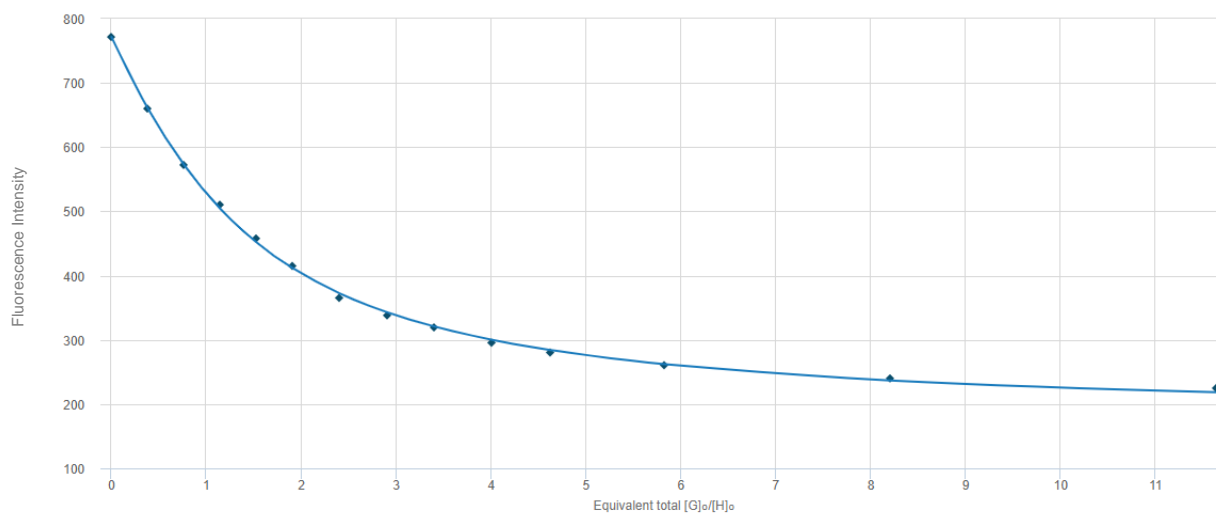


Figure S3. 1:1 binding isotherm for the fluorescence binding study of receptor **1** (11.8 μM) with uric acid **2** in H₂O at 298 K (pH = 7.4, 10 mM phosphate buffer). Emission observed at 427 nm. $K_a = 1.7 \times 10^5 \text{ M}^{-1} \pm 1.2\%$

Hypoxanthine

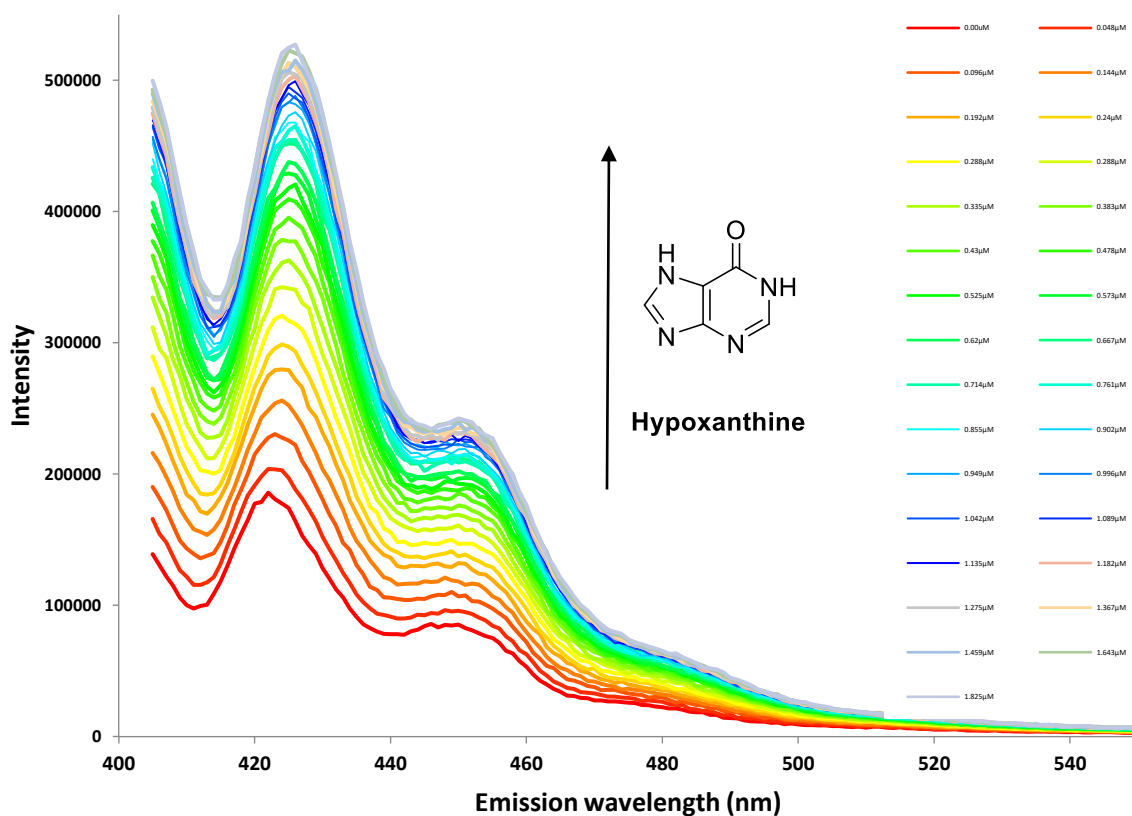


Figure S4. Fluorescence titration of receptor **1** (550 nM) with hypoxanthine **3** in H₂O (pH 7.4, 10 mM phosphate buffer) at 298K. Excitation wavelength 395nm.

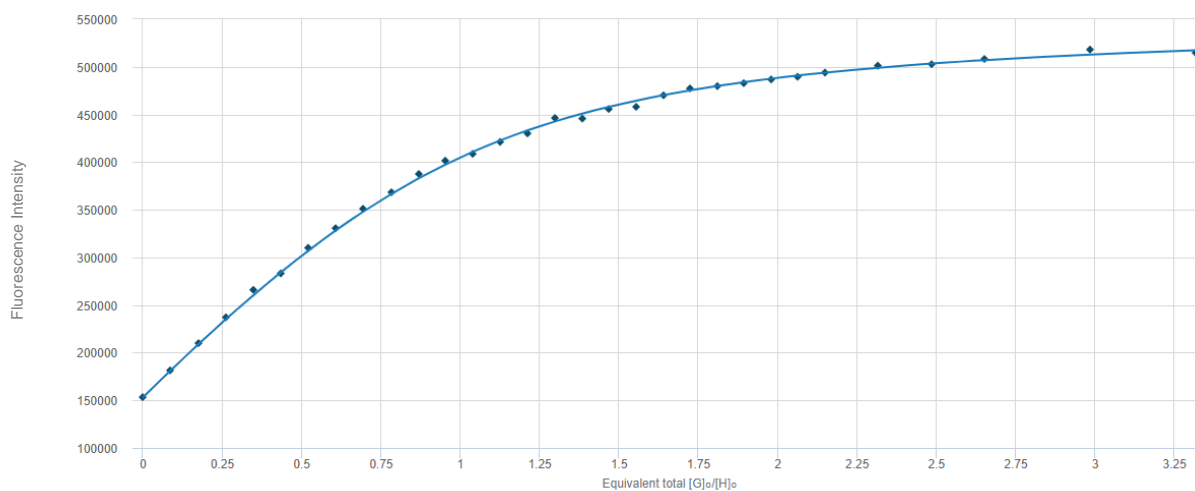


Figure S5. 1:1 binding isotherm for the fluorescence binding study of receptor **1** (550 nM) with hypoxanthine **3** in H₂O at 298 K (pH 7.4, 10 mM phosphate buffer). Emission observed at 427 nm. $K_a = 8.7 \times 10^6 \text{ M}^{-1} \pm 2.5\%$.

Caffeine

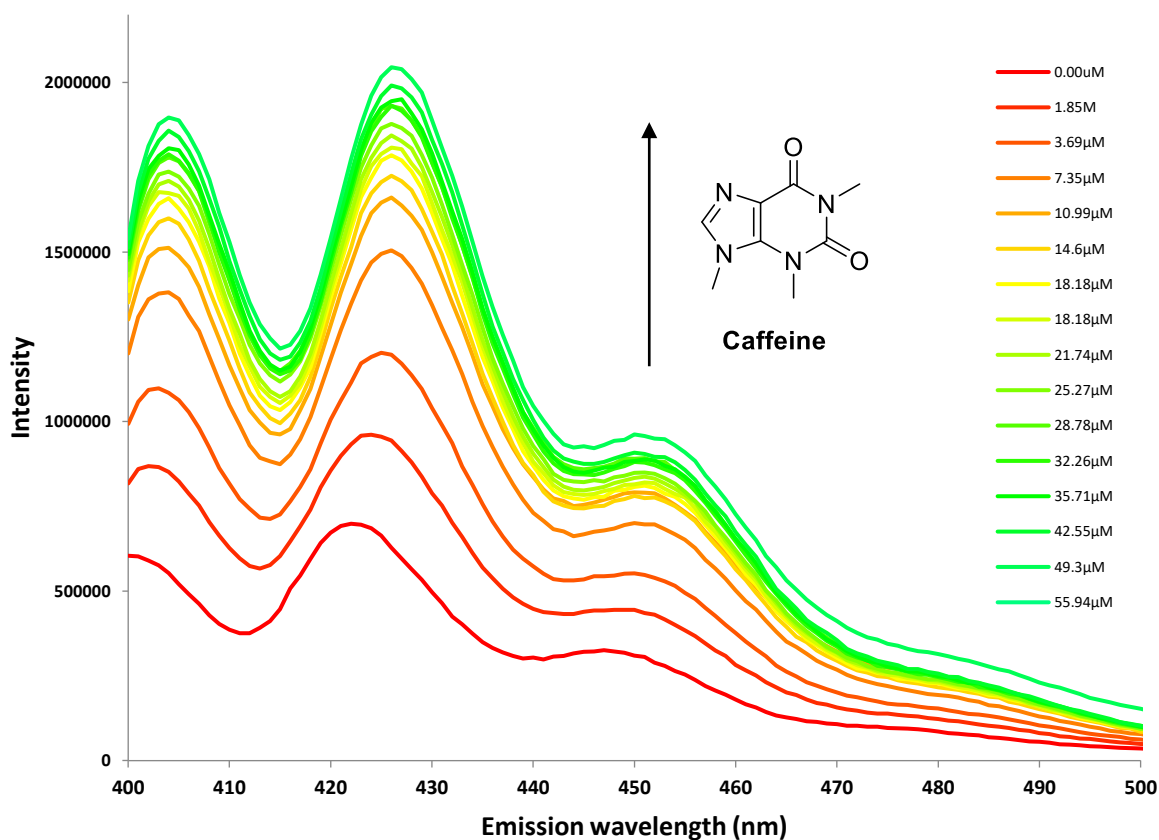


Figure S6. Fluorescence titration of receptor **1** (1.2 μM) with caffeine **4** in H₂O (pH 7.4, 10 mM phosphate buffer) at 298 K. Excitation wavelength 395 nm.

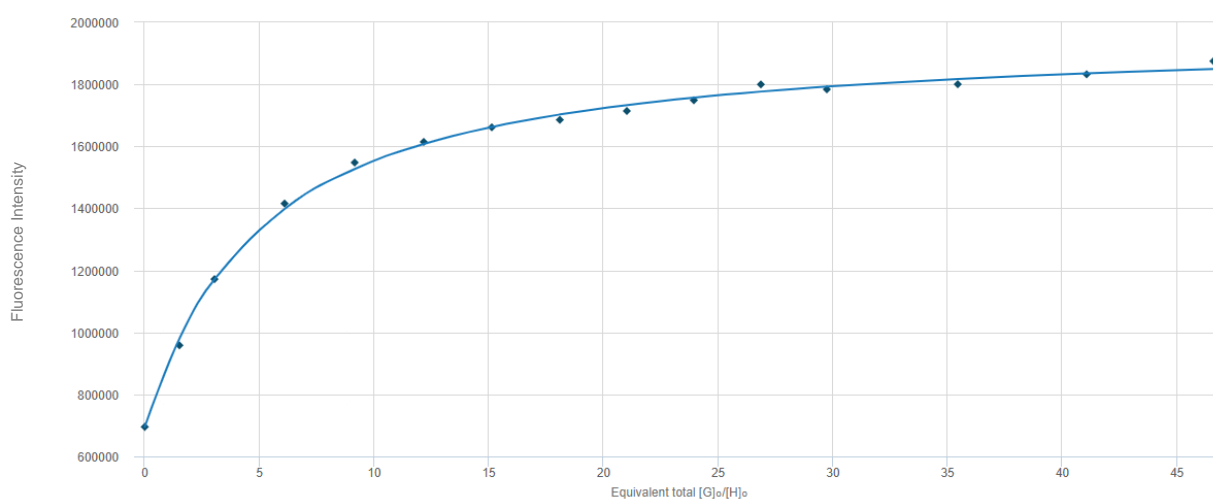


Figure S7. 1:1 binding isotherm for the fluorescence binding study of receptor **1** (1.2 μM) with caffeine **4** in H₂O (pH = 7.4, 10 mM phosphate buffer) at 298 K. Emission observed at 423 nm. $K_a = 1.7 \times 10^5 \text{ M}^{-1} \pm 1.2\%$

Theobromine

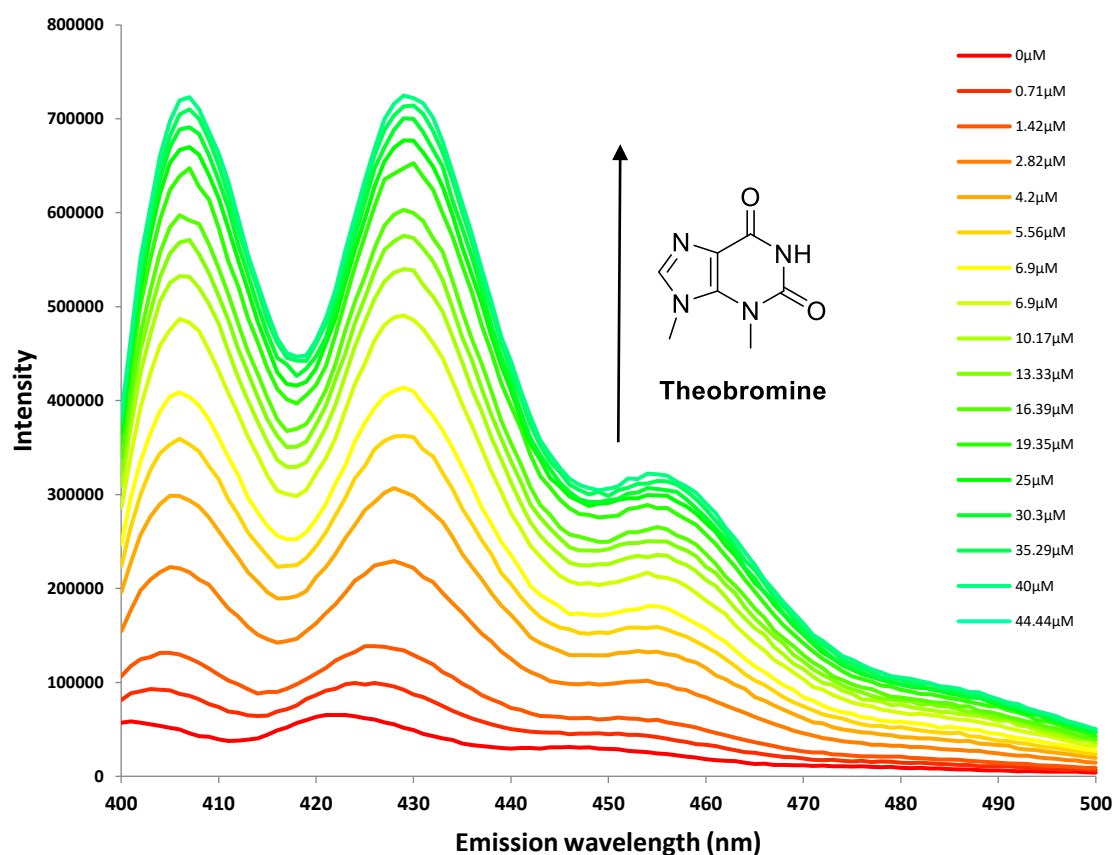


Figure S8. Fluorescence titration of receptor **1** (1.2 μM) with theobromine **5** in H₂O (pH 7.4, 10 mM phosphate buffer) at 298 K. Excitation wavelength 395 nm.

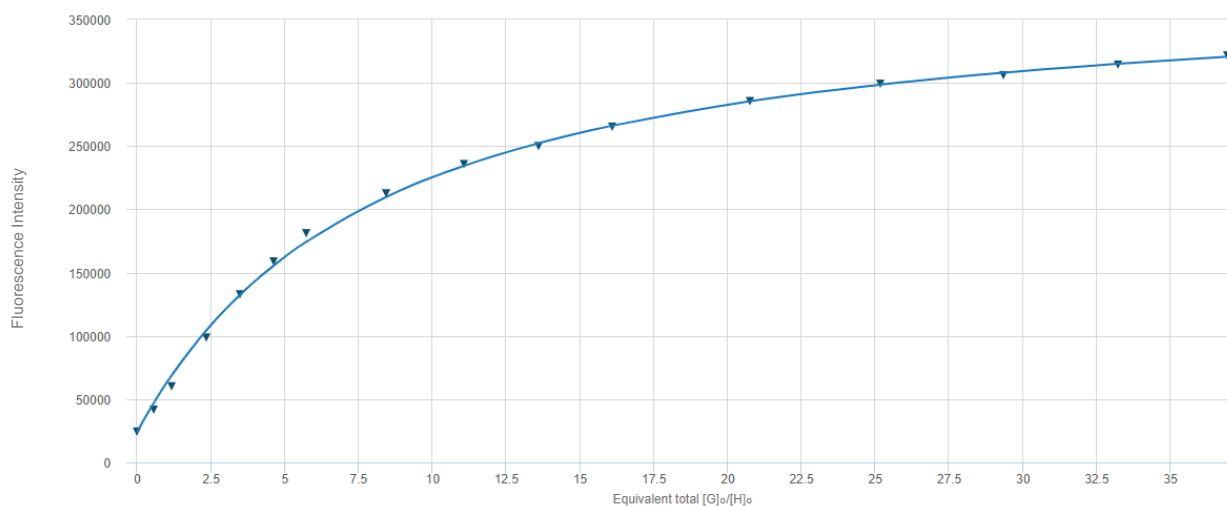


Figure S9. 1:1 binding isotherm for the fluorescence binding study of receptor **1** (1.2 μM) with theobromine **5** in H₂O (pH = 7.4, 10 mM phosphate buffer) at 298 K. Emission observed at 427 nm. $K_a = 1.1 \times 10^5 \text{ M}^{-1} \pm 3.5\%$.

Adenine

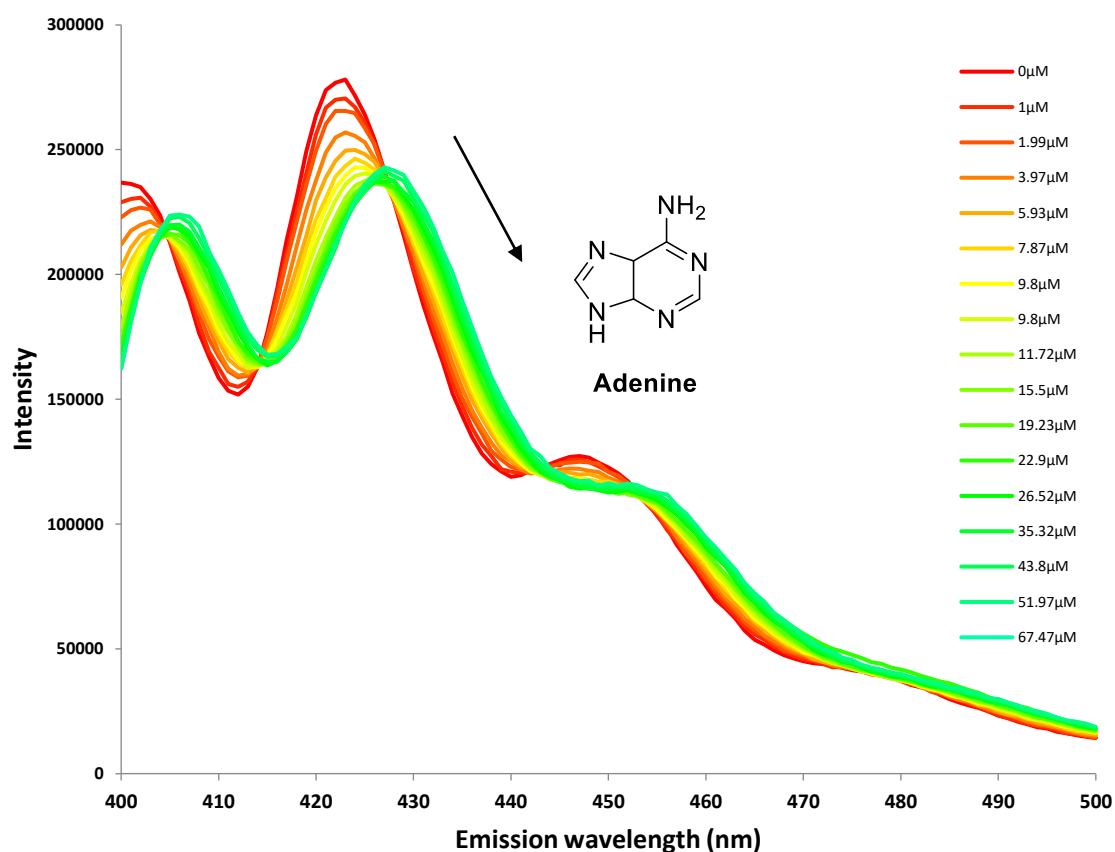


Figure S10. Fluorescence titration of receptor **1** (500 nM) with adenine **6** in H₂O (pH 7.4, 10 mM phosphate buffer) at 298 K. Excitation wavelength 395 nm.

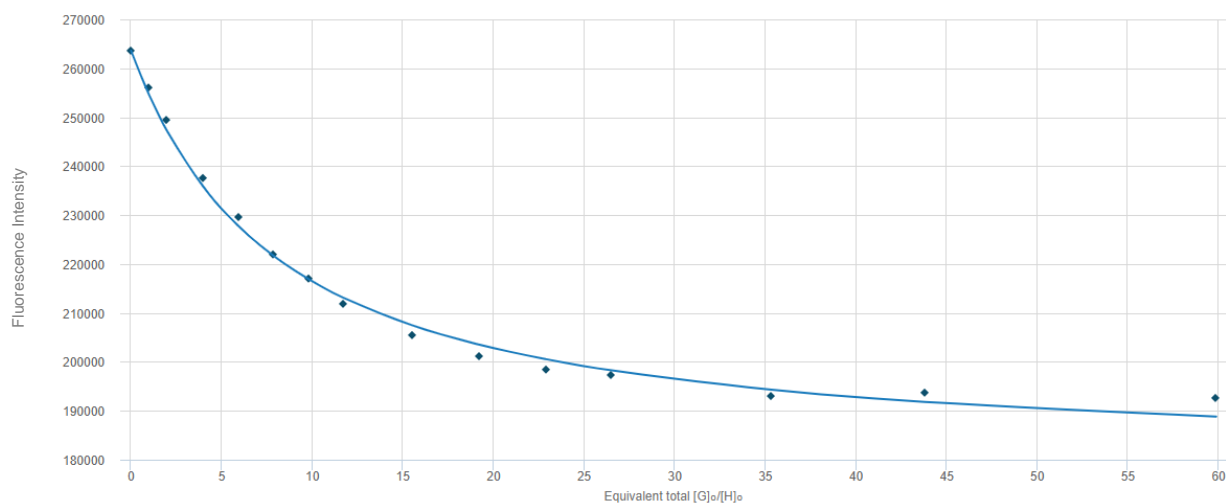


Figure S11. 1:1 binding isotherm for the fluorescence binding study of receptor **1** (500 nM) with adenine **6** in H₂O (pH 7.4, 10 mM phosphate buffer) at 298 K. Emission observed at 419 nm. $K_a = 1.3 \times 10^5 \text{ M}^{-1} \pm 7.4\%$.

Thymine

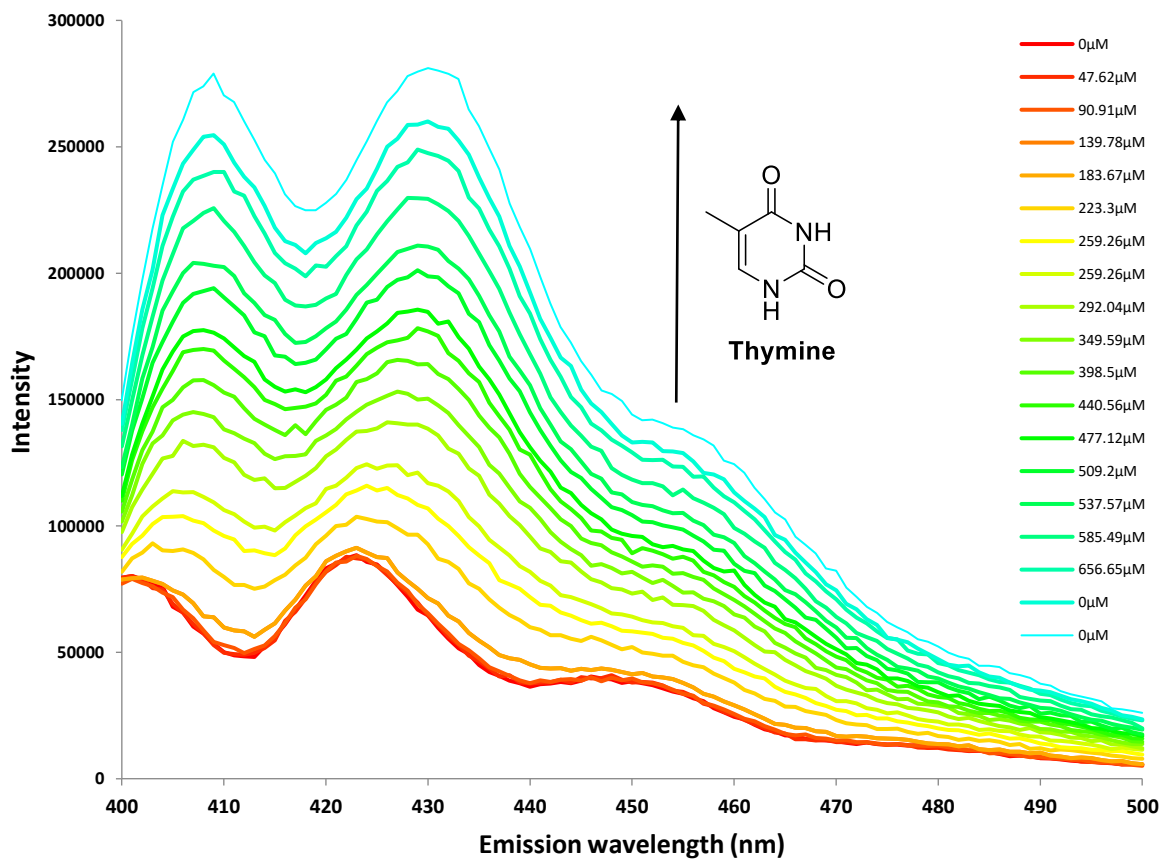


Figure S12. Fluorescence titration of receptor **1** (1.2 μM) with thymine **7** in H₂O (pH 7.4, 10 mM phosphate buffer) at 298 K. Excitation wavelength 395 nm.

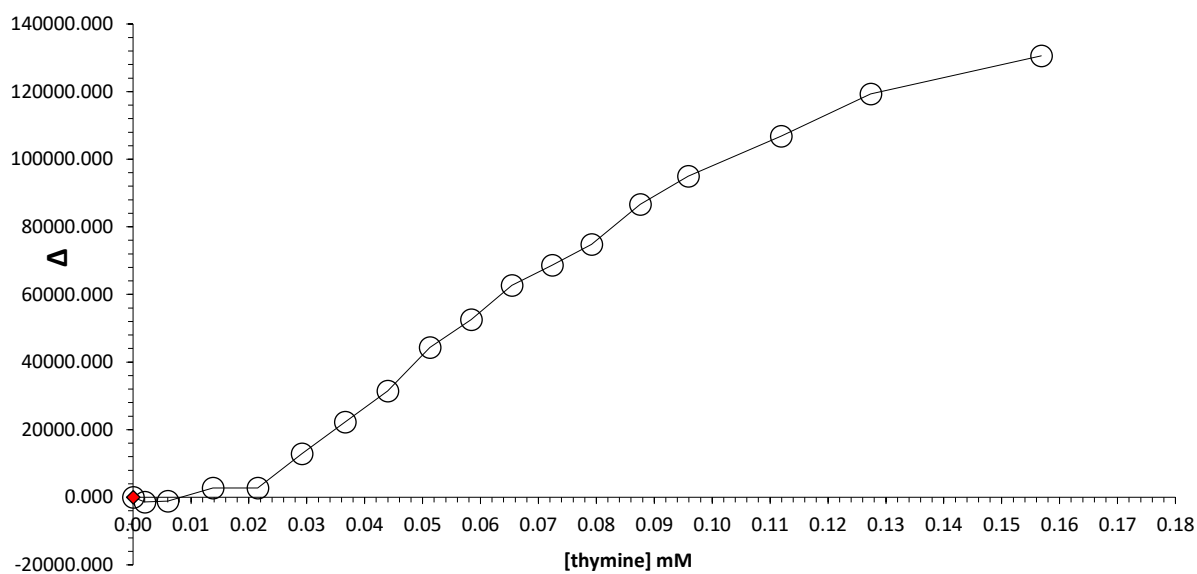


Figure S13. Binding isotherm produced from the fluorescence titration of receptor **1** with thymine **7**. The shape of the curve suggests 1:1 + 1:2 stoichiometry.

Uracil

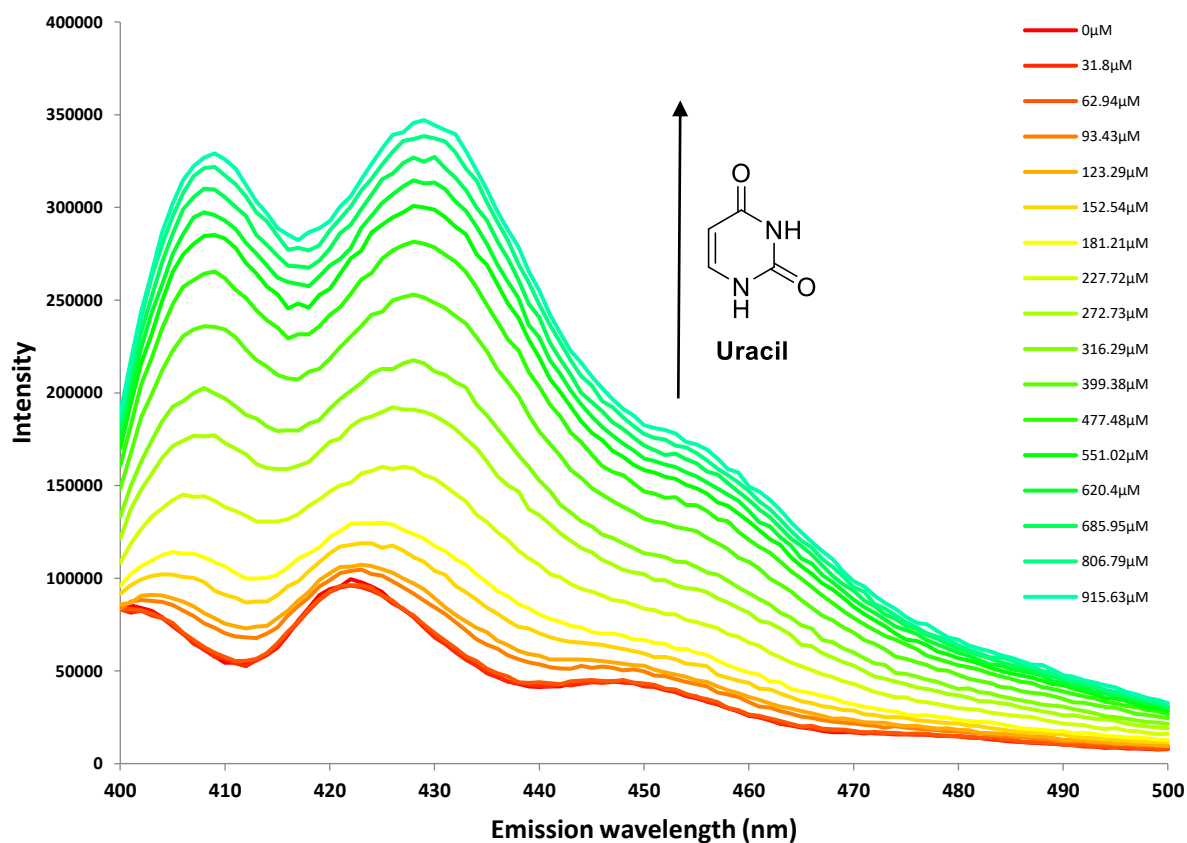


Figure S14. Fluorescence titration of receptor **1** (1 μM) with uracil **8** in H_2O (pH 7.4, 10 mM phosphate buffer) at 298 K. Excitation wavelength 395 nm.

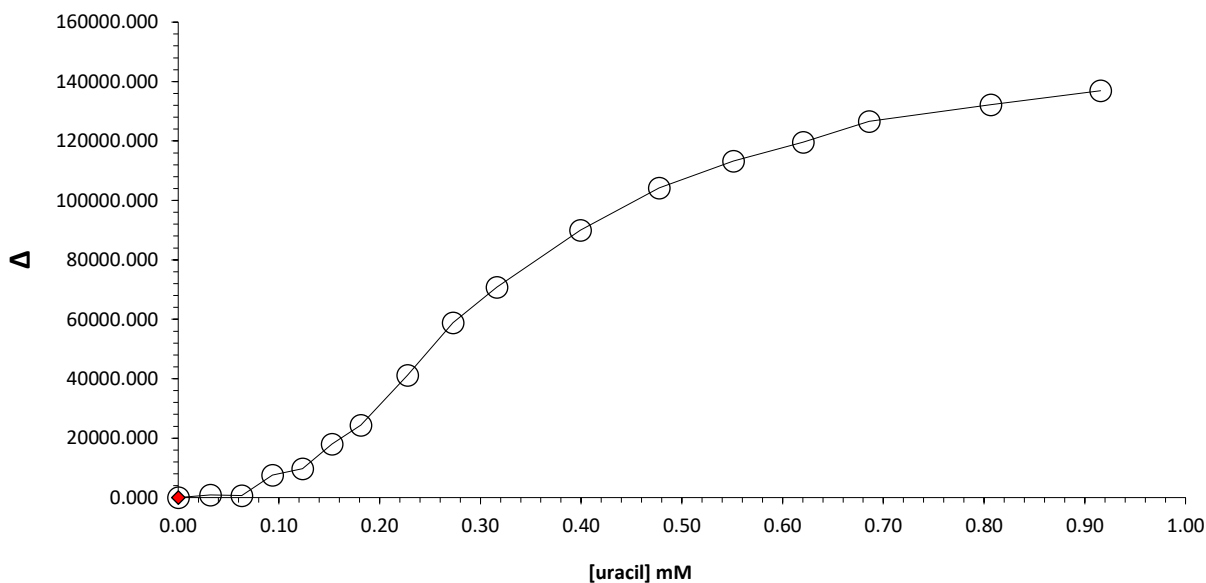


Figure S15. Binding isotherm produced from the fluorescence titration of receptor **1** with uracil **8**. The shape of the curve suggests 1:1 + 1:2 stoichiometry.

Cytosine

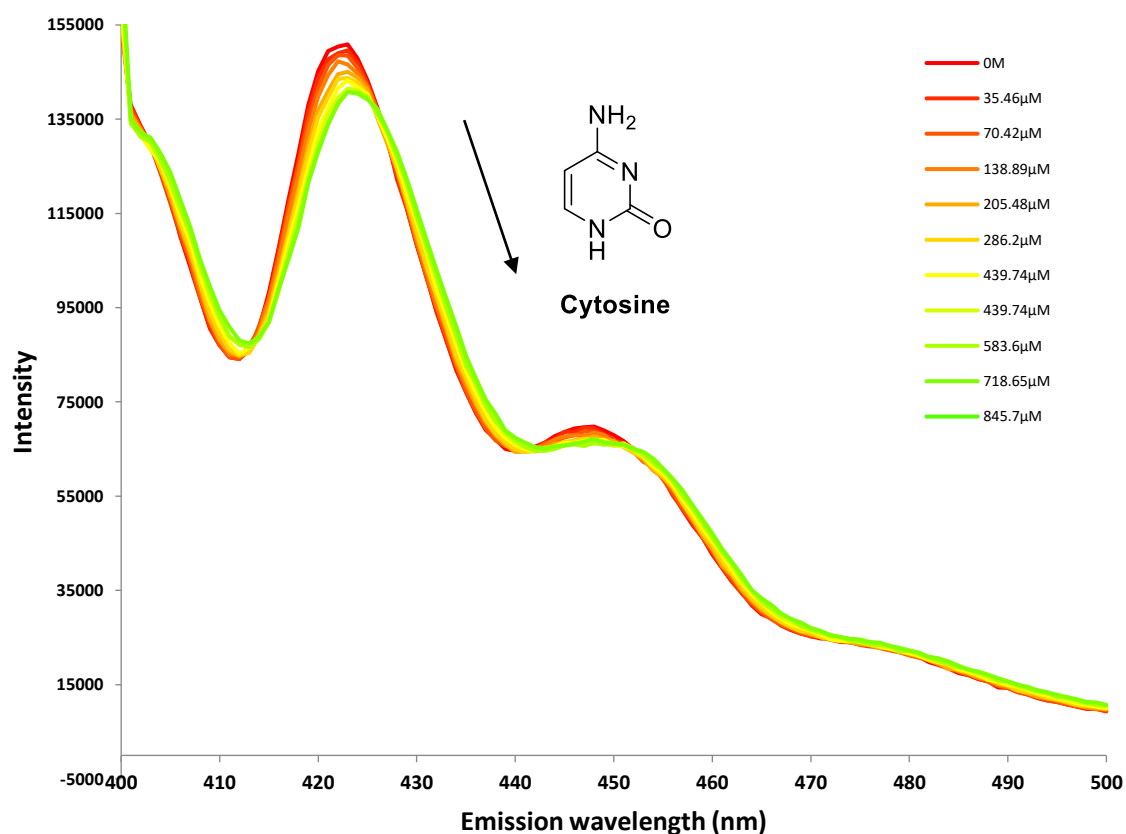


Figure S16. Fluorescence titration of receptor **1** (1 μM) with cytosine **9** in H₂O (pH 7.4, 10 mM phosphate buffer) at 298 K. Excitation wavelength 395 nm.

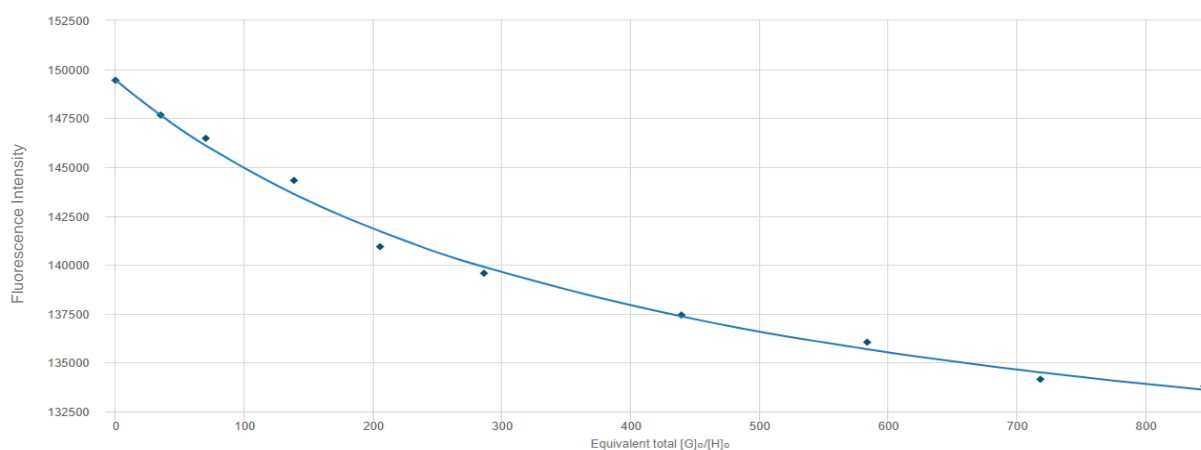


Figure S17. 1:1 binding isotherm for the fluorescence binding study of receptor **1** (500 nM) with cytosine **9** in H₂O (pH 7.4, 10 mM phosphate buffer) at 298 K. Emission observed at 419 nm. $K_a = 2.3 \times 10^3 \text{ M}^{-1} \pm 7.6\%$.

Adenosine Triphosphate (ATP)

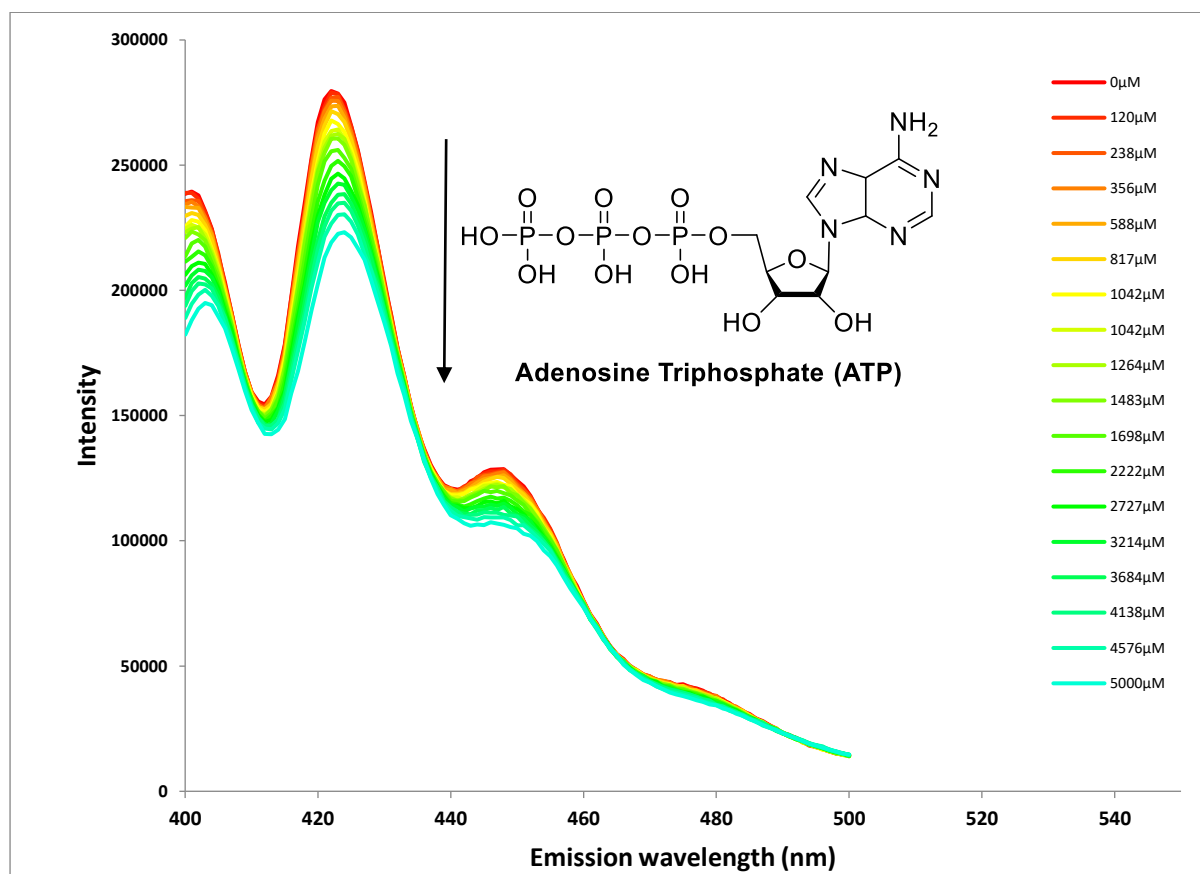


Figure S18. Fluorescence titration of receptor **1** (1 μM) with adenosine triphosphate (ATP) **10** in H₂O (pH 7.4, 10 mM phosphate buffer) at 298 K. Excitation wavelength 395 nm.

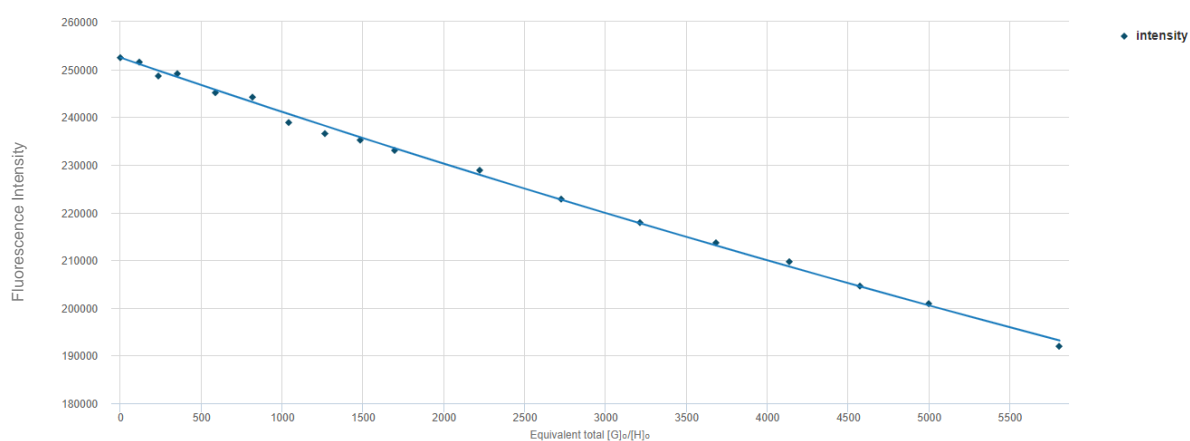


Figure S19. 1:1 binding isotherm for the fluorescence binding study of receptor **1** (500 nM) with adenosine triphosphate (ATP) **10**. Emission observed at 419 nm. $K_a = 24 \text{ M}^{-1} \pm 1.8\%$.

^1H NMR Binding Studies

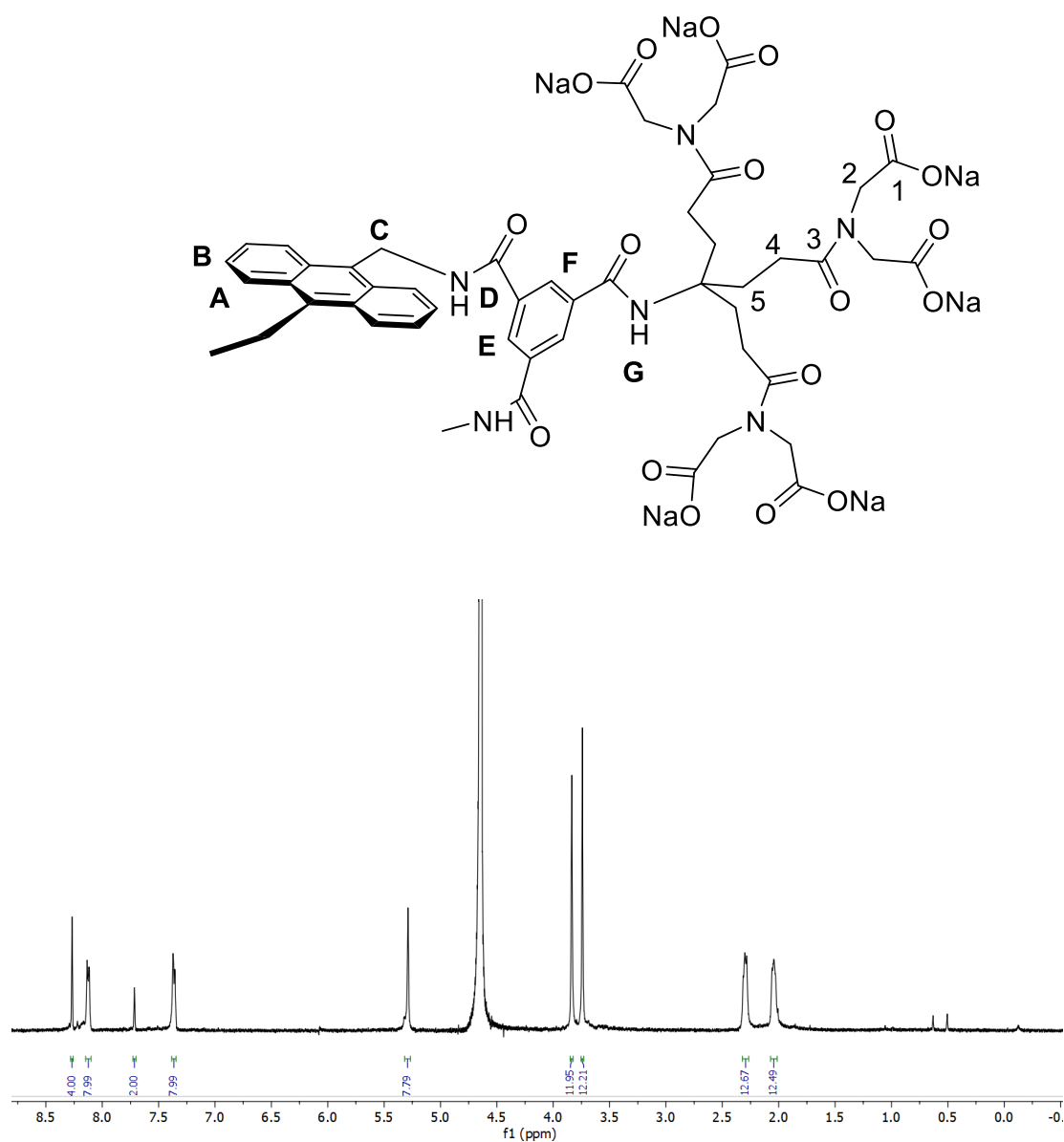


Figure S20: ^1H NMR spectrum of receptor **1** (500 MHz, D_2O), with labelling system: 8.50 (s, 4H, CF-H), 8.33 (m, 8H, CB-H), 7.90 (s, 2H, CE-H), 7.57 (m, 8H, CA-H), 5.29 (s, 4H, CC-H), 4.04/3.95 (2s, 24H, C2-H_2), 2.5 (t, $J = 6.5$ Hz, 12H, C4-H_2), 2.24 (t, $J = 6.5$ Hz, 12H, C5-H_2). The signals for ND-H and NG-H are visible in spectra taken in $\text{H}_2\text{O}/\text{D}_2\text{O}$ (9:1), see for example Fig S22.

Uric Acid

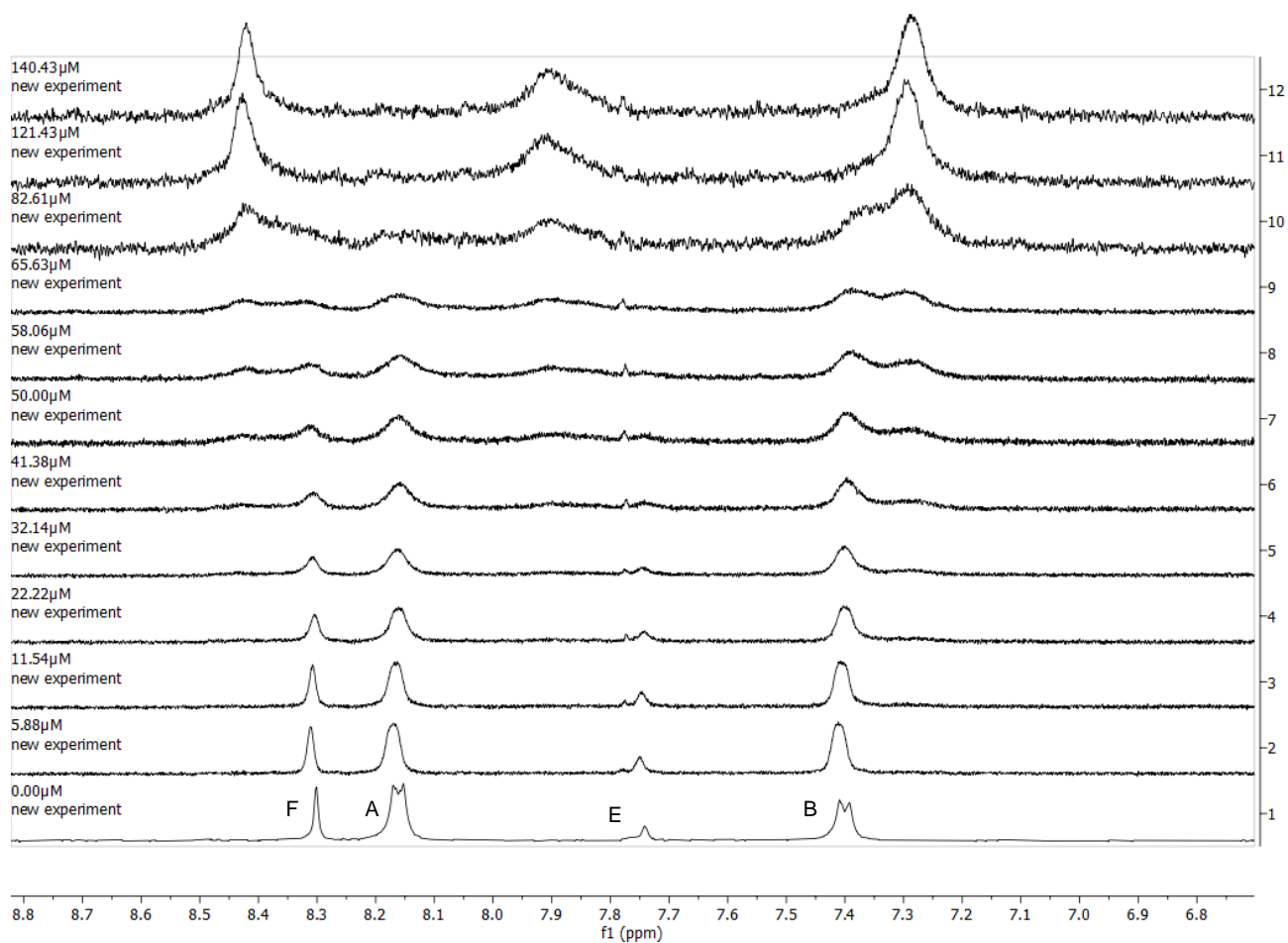


Figure S21. Partial ^1H NMR spectra from the titration of receptor **1** (75 μM) with uric acid **2** in D_2O (10 mM phosphate buffer, pH 7.4) at 298 K.

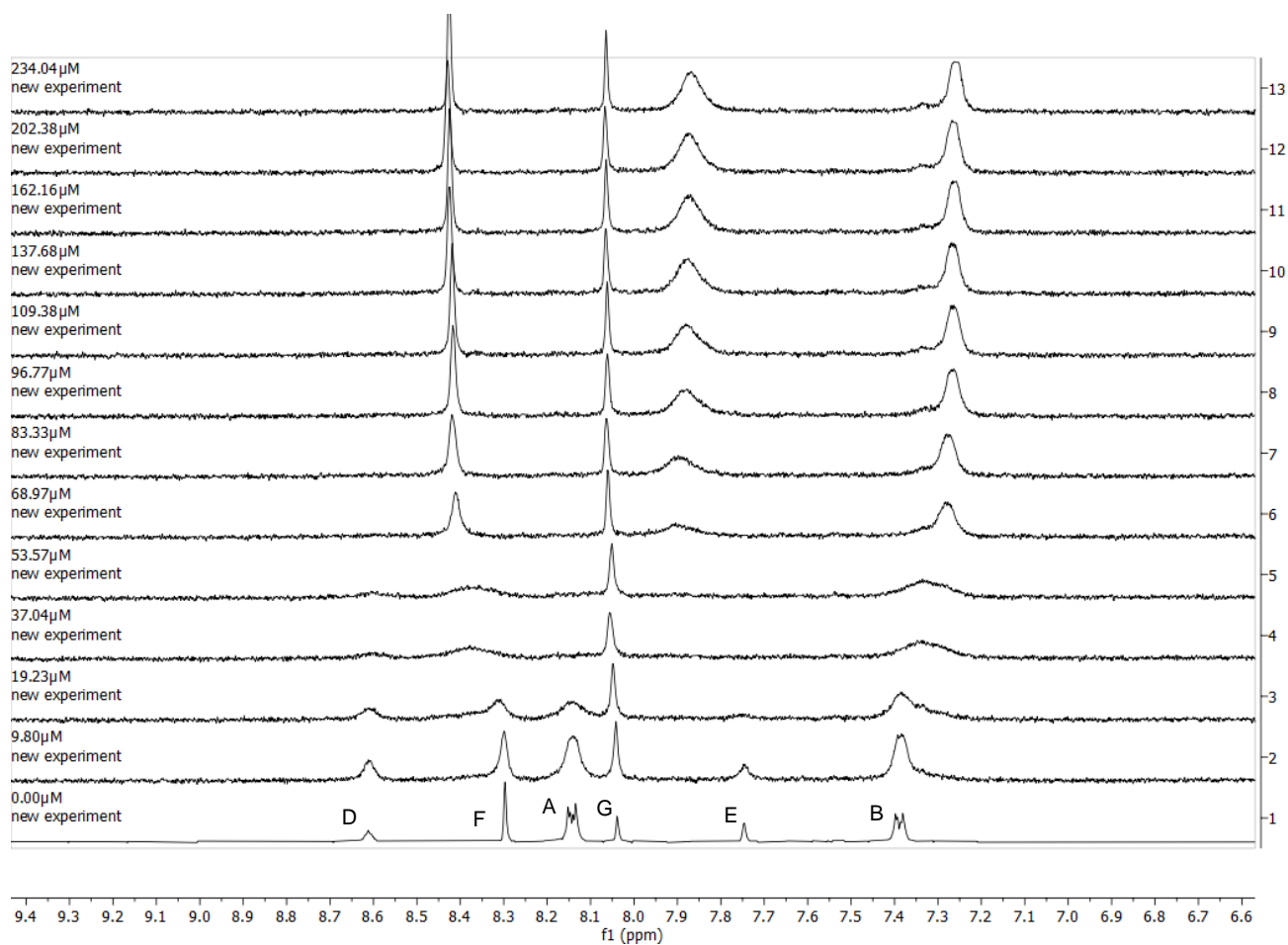


Figure S22. Partial ^1H NMR spectra from the titration of receptor **1** ($75\ \mu\text{M}$) with uric acid **2** in $\text{H}_2\text{O}/\text{D}_2\text{O}$ (9:1, 10 mM phosphate buffer, pH 7.4) at 298 K. Unfortunately the lactam NH signals D broaden during the titration and do not reappear.

Hypoxanthine

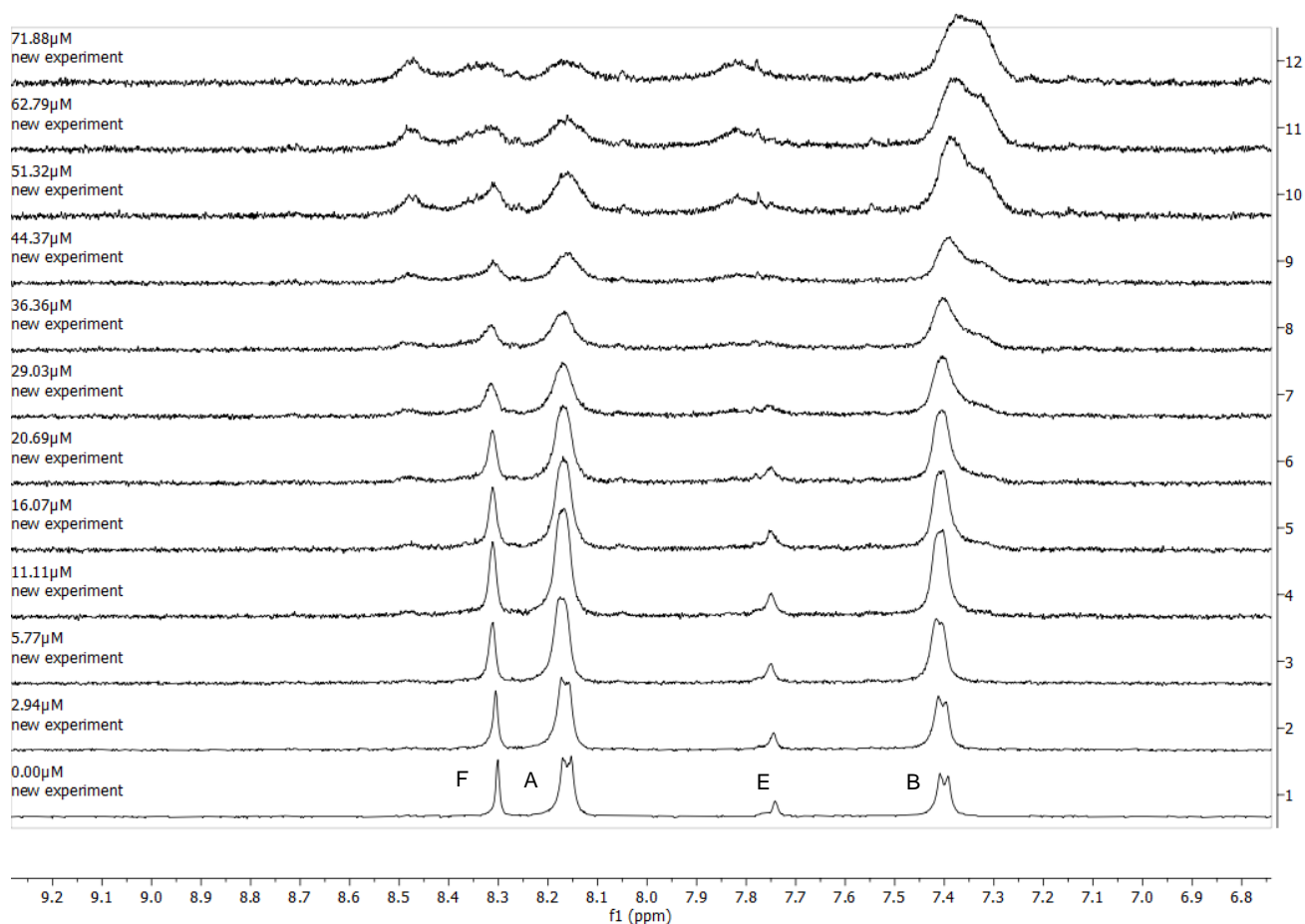


Figure S23. Partial ^1H NMR spectra from the titration of receptor **1** (75 μM) with hypoxanthine **3** in D_2O (10 mM phosphate buffer, pH 7.4) at 298 K.

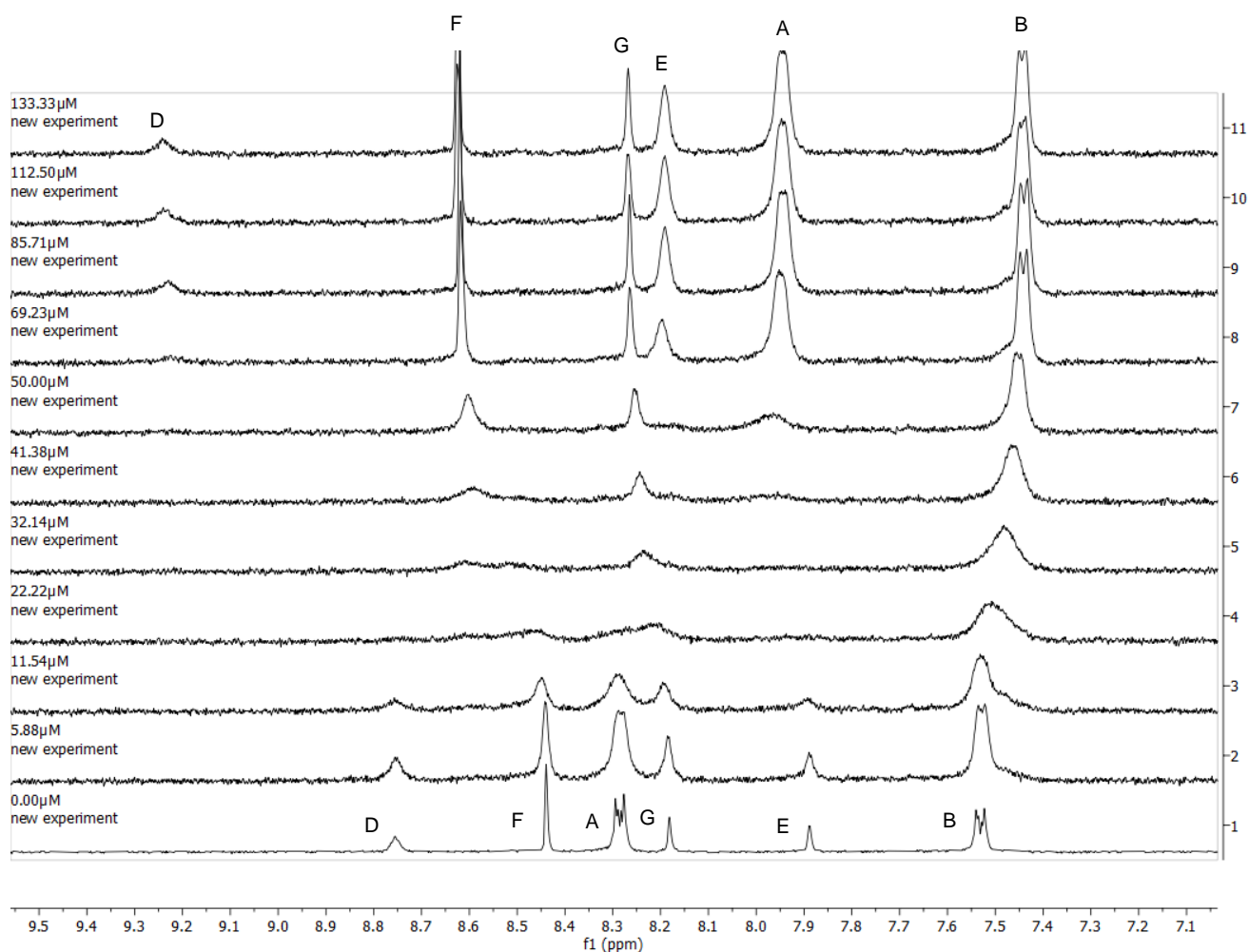


Figure S24. Partial ^1H NMR spectra from the titration of receptor **1** (100 μM) with hypoxanthine **3** in $\text{H}_2\text{O}/\text{D}_2\text{O}$ (9:1, 10 mM phosphate buffer, pH 7.4) at 298 K. The assignments in the complex are based on peak shapes, integrations and movements where observable.

Caffeine

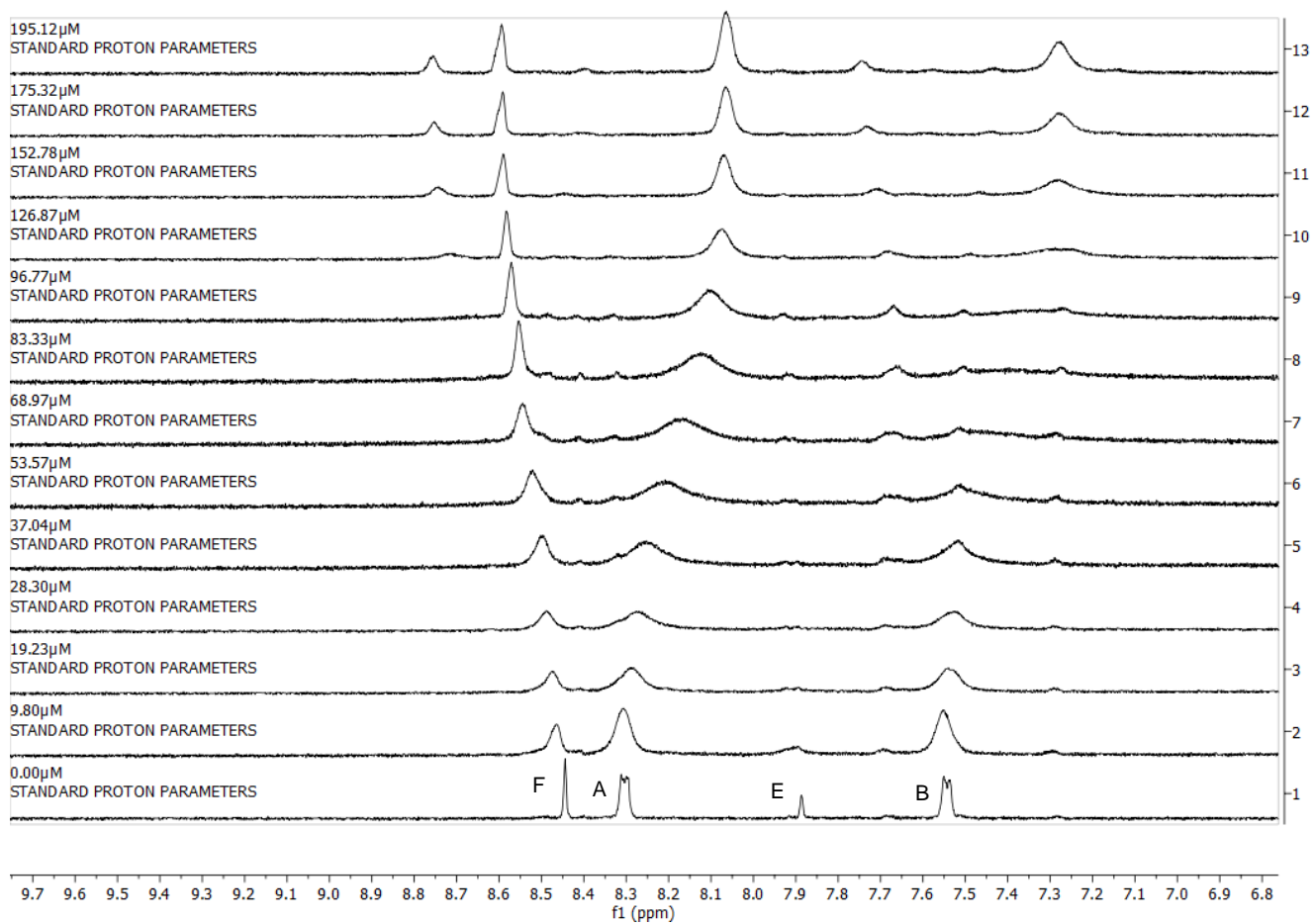


Figure S25. Partial ^1H NMR spectra from the titration of receptor **1** (75 μM) with caffeine **4** in D_2O (10 mM phosphate buffer, pH 7.4) at 298 K.

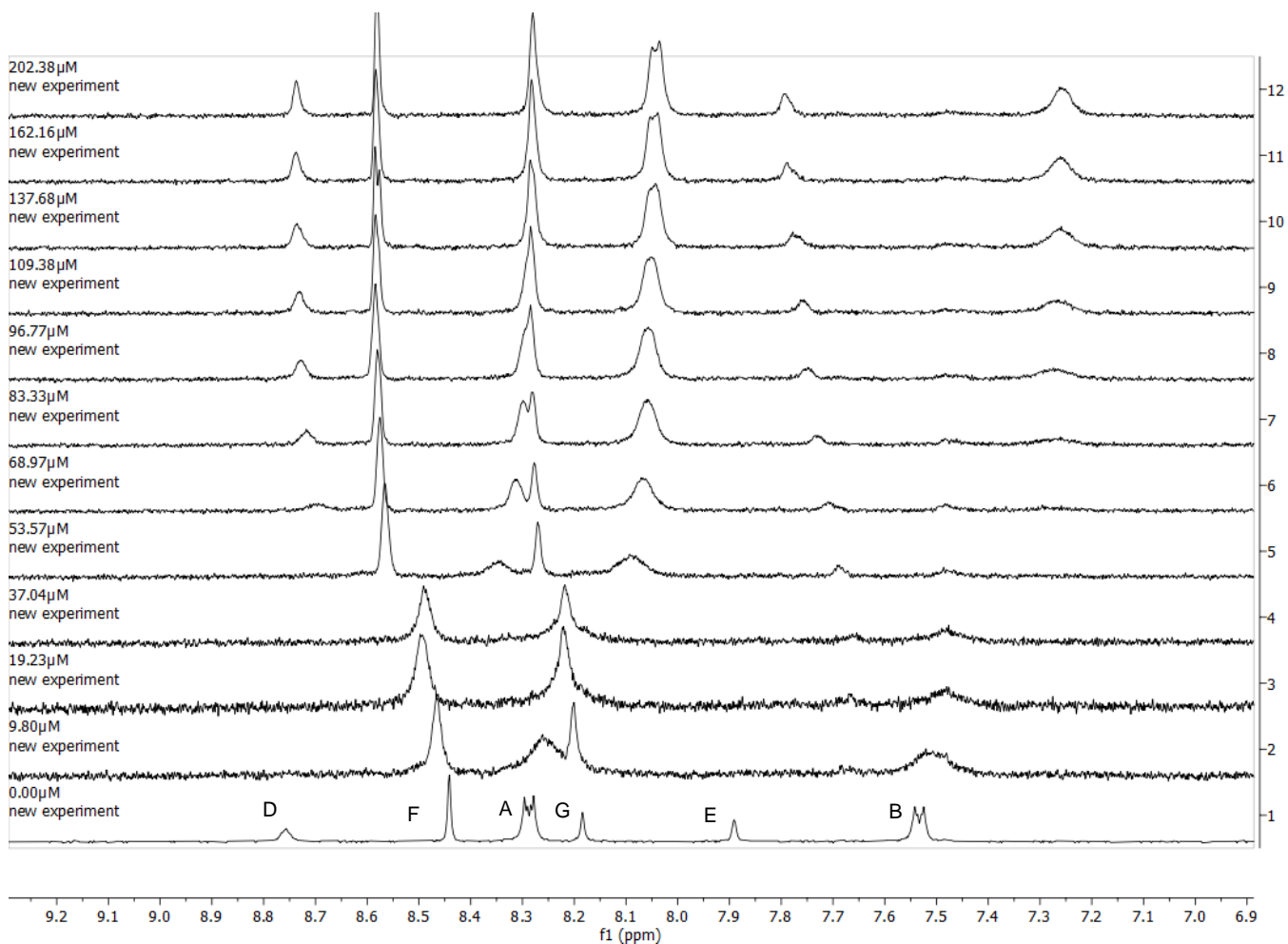


Figure S26. Partial ¹H NMR spectra from the titration of receptor **1** (100 μM) with caffeine **4** in H₂O/D₂O (9:1, 10 mM phosphate buffer, pH 7.4) at 298 K.

Thymine

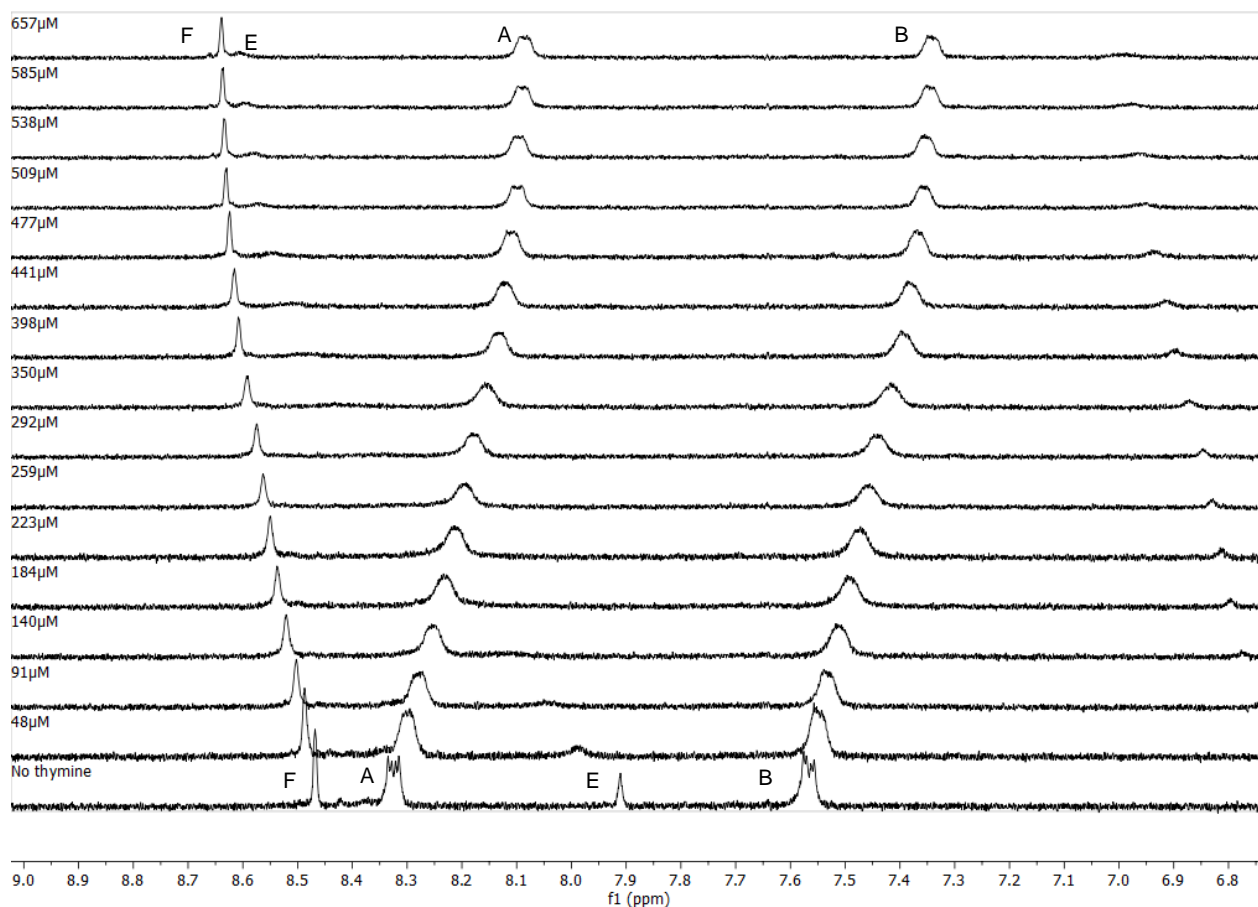


Figure S27. Partial ^1H NMR spectra from the titration of receptor **1** (0.5 mM) with thymine **7** in D_2O (10 mM phosphate buffer, pH 7.4) at 298 K.

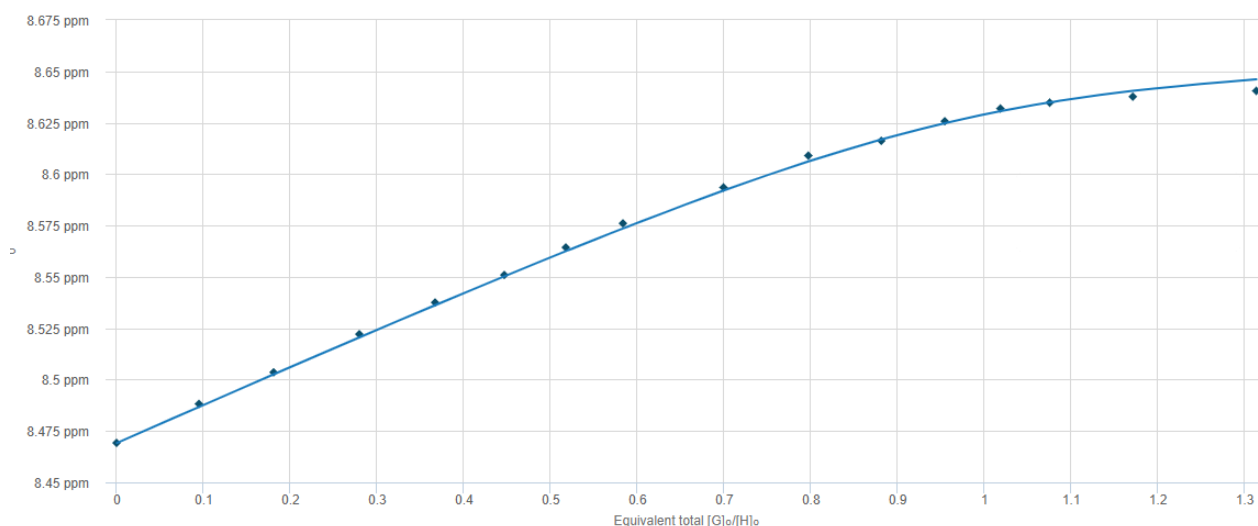


Figure S28. 1:1 binding isotherm for the ^1H NMR binding study of receptor **1** (500 nM) with thymine **7** in D_2O phosphate buffer (10 mM, pH 7.4) at 298 K, tracking proton F. $K_a = 5.8 \times 10^5 \text{ M}^{-1} \pm 12.7\%$.

Uracil

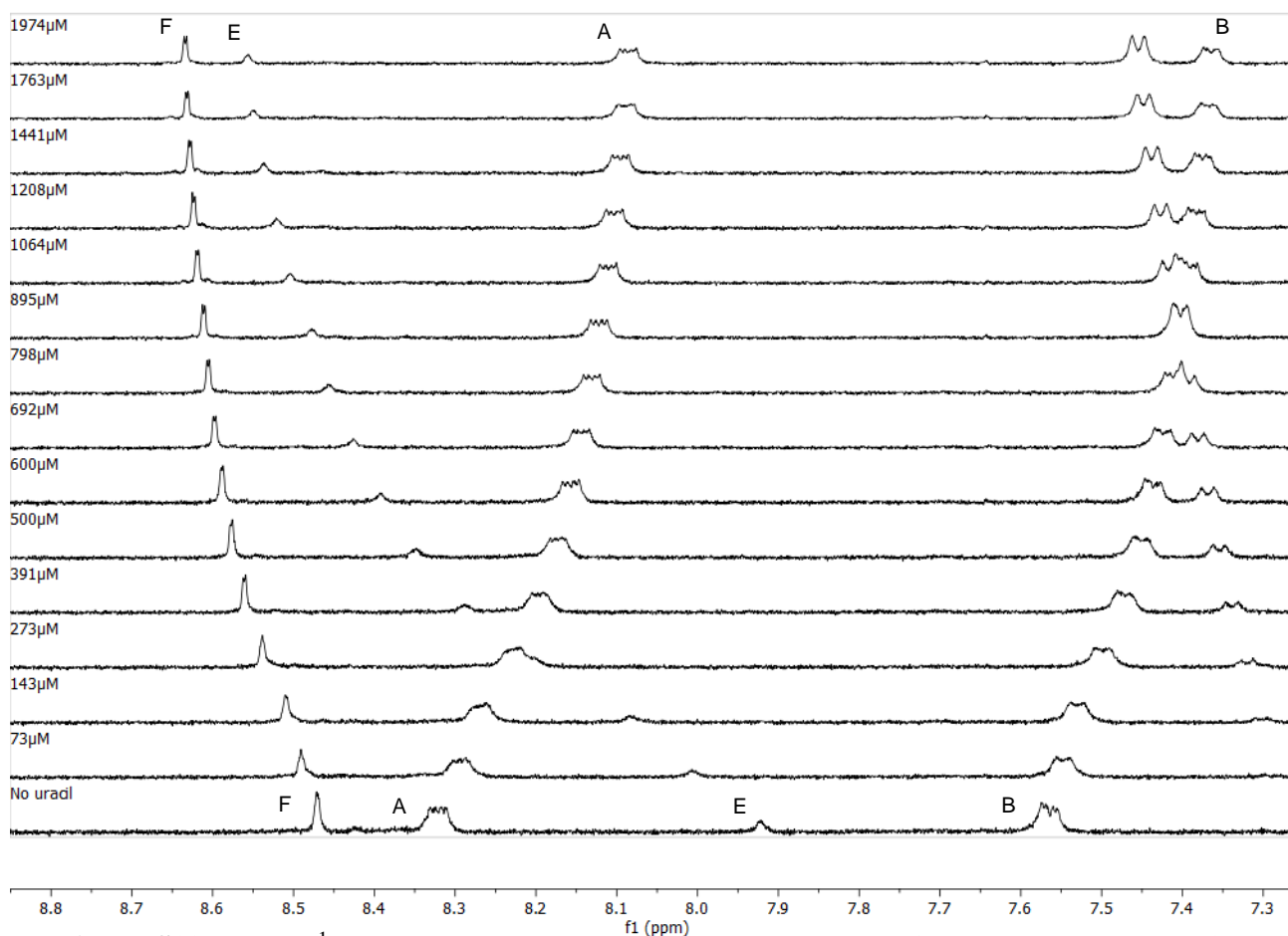


Figure S29. Partial ^1H NMR spectra from the titration of receptor **1** (0.5 mM) with uracil **8** in D_2O (10 mM phosphate buffer) at 298 K.

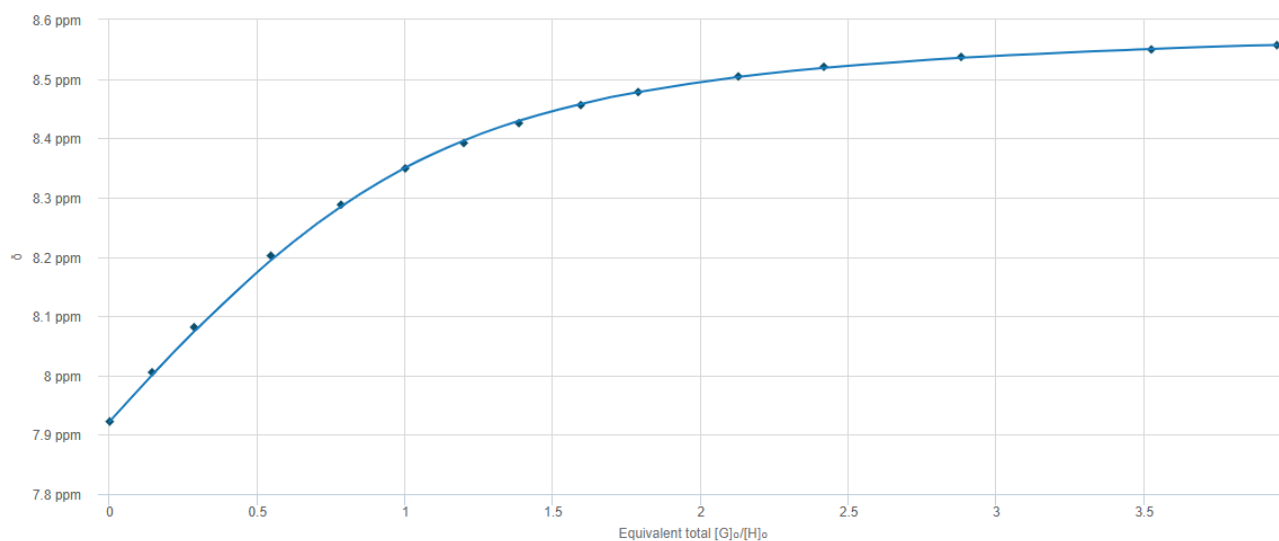


Figure S30. 1:1 binding isotherm for the ^1H NMR binding study of receptor **1** (500 nM) with uracil **8** in D_2O (10 mM phosphate buffer, pH 7.4) at 298 K, tracking proton E. $K_a = 9.1 \times 10^3 \text{ M}^{-1} \pm 3.0\%$.

Isothermal Titration Microcalorimetry (ITC)

Uric Acid

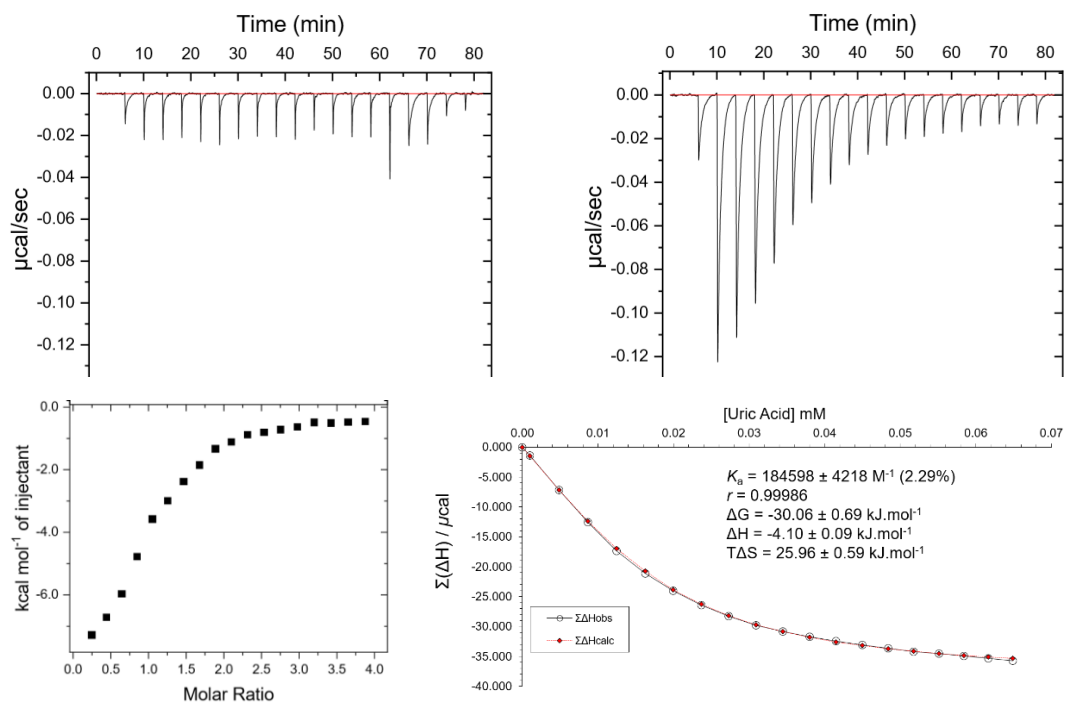


Figure S31. ITC binding results for receptor **1** (20 µM) titrated with uric acid **2** (400 µM) in 10 mM phosphate buffer solution (pH 7.4), in which: (Top, Left) Blank run (addition of uric acid into phosphate buffer); (Top, Right) The titration (uric acid into receptor **1**); (Bottom, Left) Plot of change in enthalpy vs molar ratio and (Bottom, Right) fitting curve using an Excel spreadsheet ($K_a = 184598 \pm 4218 \text{ M}^{-1}$).

Hypoxanthine

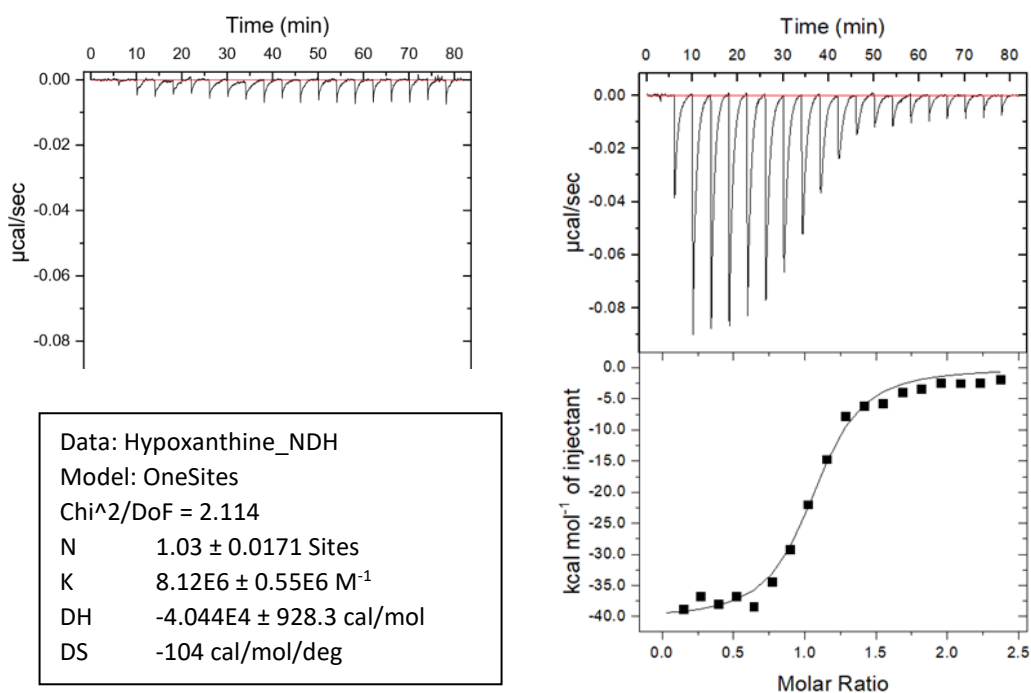


Figure S32. ITC binding results for receptor **1** (4.5 µM) titrated with hypoxanthine **3** (55 µM) in 10 mM phosphate buffer solution (pH 7.4), in which: (Top, Left) Blank run (addition of hypoxanthine into phosphate buffer); (Top, Right) The titration (hypoxanthine into receptor **1**); (Bottom, Right) Fitting curve — data fitted to 1:1 binding model ($K_a = (8.12 \times 10^6 \text{ M}^{-1})$); (Bottom, Left) Thermodynamic parameters for hypoxanthine binding to receptor **1**.

Caffeine

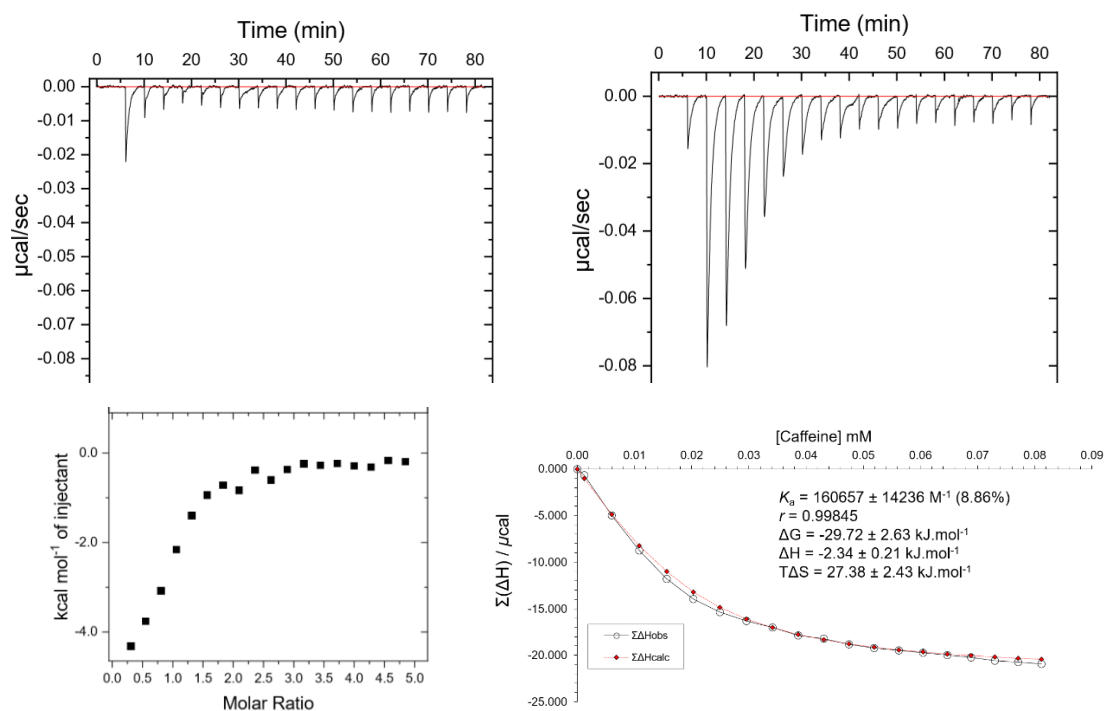


Figure S33. ITC binding results for receptor **1** (20 μM) titrated with caffeine **4** (500 μM) in 10 mM phosphate buffer solution (pH 7.4), in which: (Top, Left) Blank run (addition of caffeine into phosphate buffer); (Top, Right) The titration (caffeine into receptor **1**); (Bottom, Left) Plot of change in enthalpy vs molar ratio and (Bottom, Right) fitting curve using an Excel spreadsheet ($K_a = 160657 \pm 14236 \text{ M}^{-1}$).

Molecular Modelling

Modelling studies employed Maestro Version 10.4.018, using Batchmin V11.0 for energy minimisation. For the 1:1 complexes of **1** with purines **2-6** and cytosine **9**, Monte Carlo Molecular Mechanics (MCMM) simulations were undertaken allowing guests to move and rotate within the binding site. The calculations employed the OPLS2005 force field, aqueous GB/SA solvation, and 1000 MCMM steps. Figs S34-S38 and S41 show the resulting ground state conformations. For the 1:2 complexes of **1** with thymine **7** and uracil **8** the guests were moved into place by hand before minimisation, as MCMM caused one guest to leave the cavity. The results are presented in Figs S39 and S40.

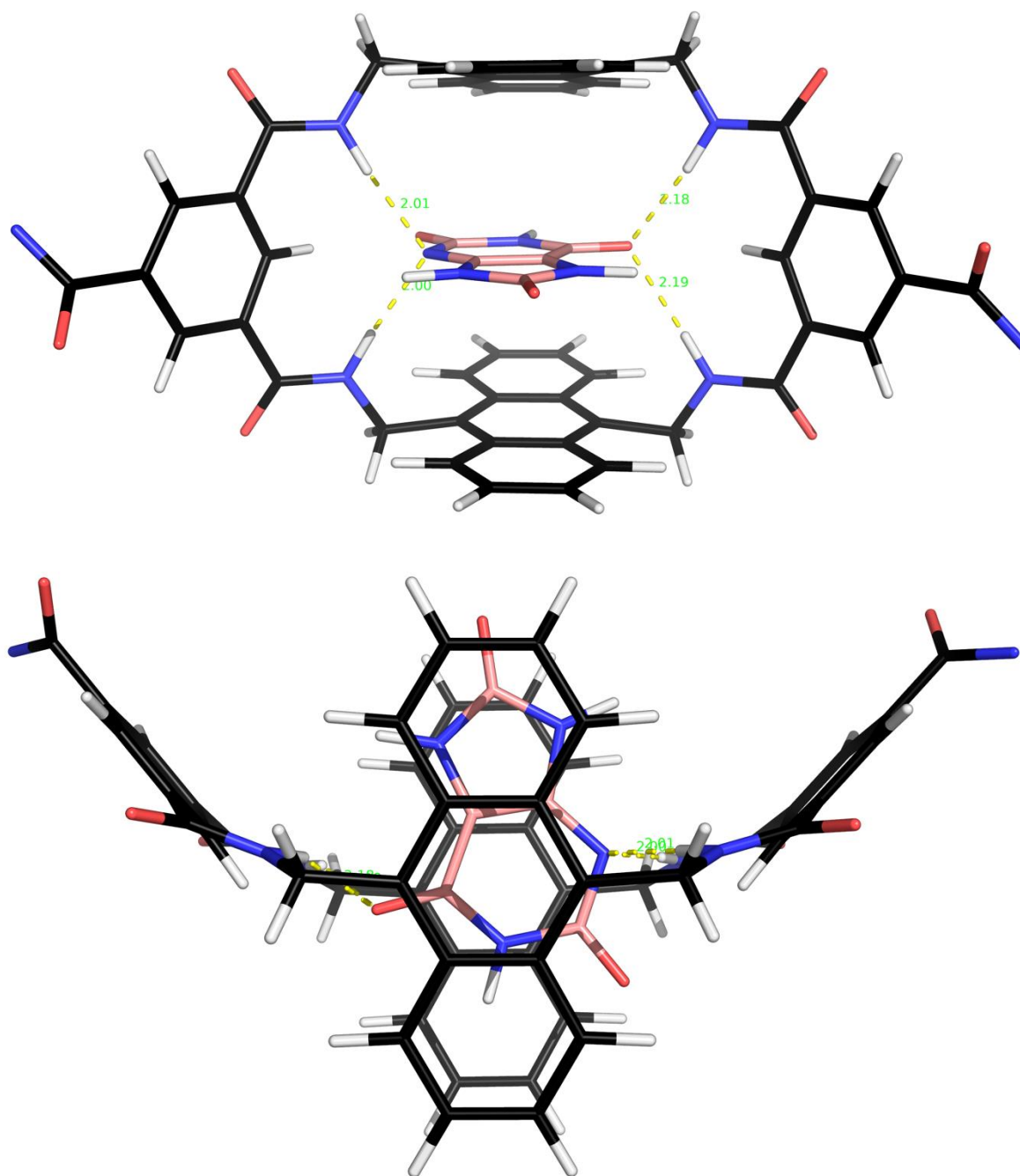


Figure S34. Model of uric acid monoanion **2** bound to receptor **1**, shown from two perspectives. Intermolecular hydrogen bonds are shown as yellow dashed lines. Side-chains are omitted for clarity.

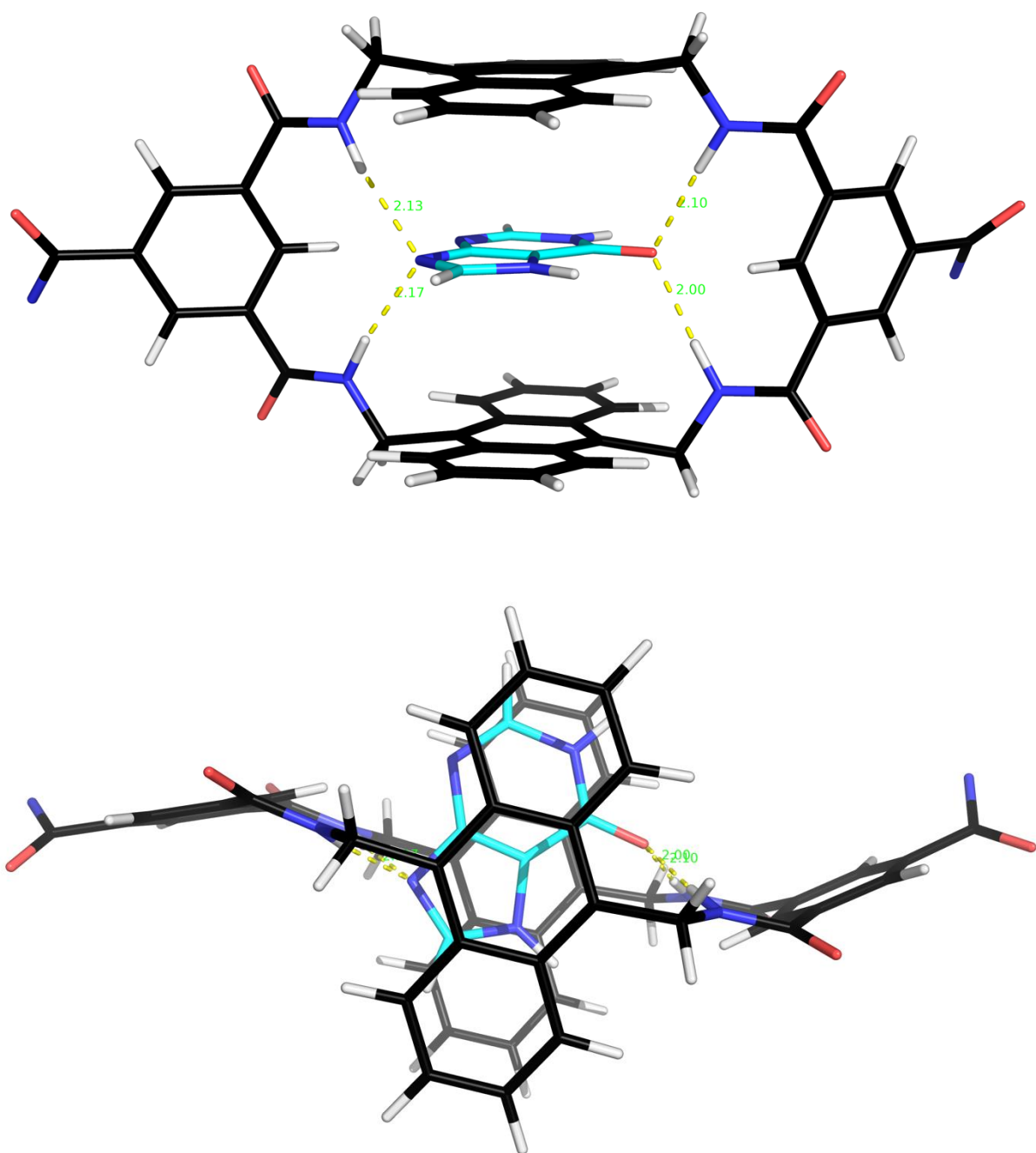


Figure S35. Model of hypoxanthine **3** bound to receptor **1**, shown from two perspectives. Side-chains are omitted for clarity. Intermolecular hydrogen bonds are shown as yellow dashed lines. Side-chains are omitted for clarity.

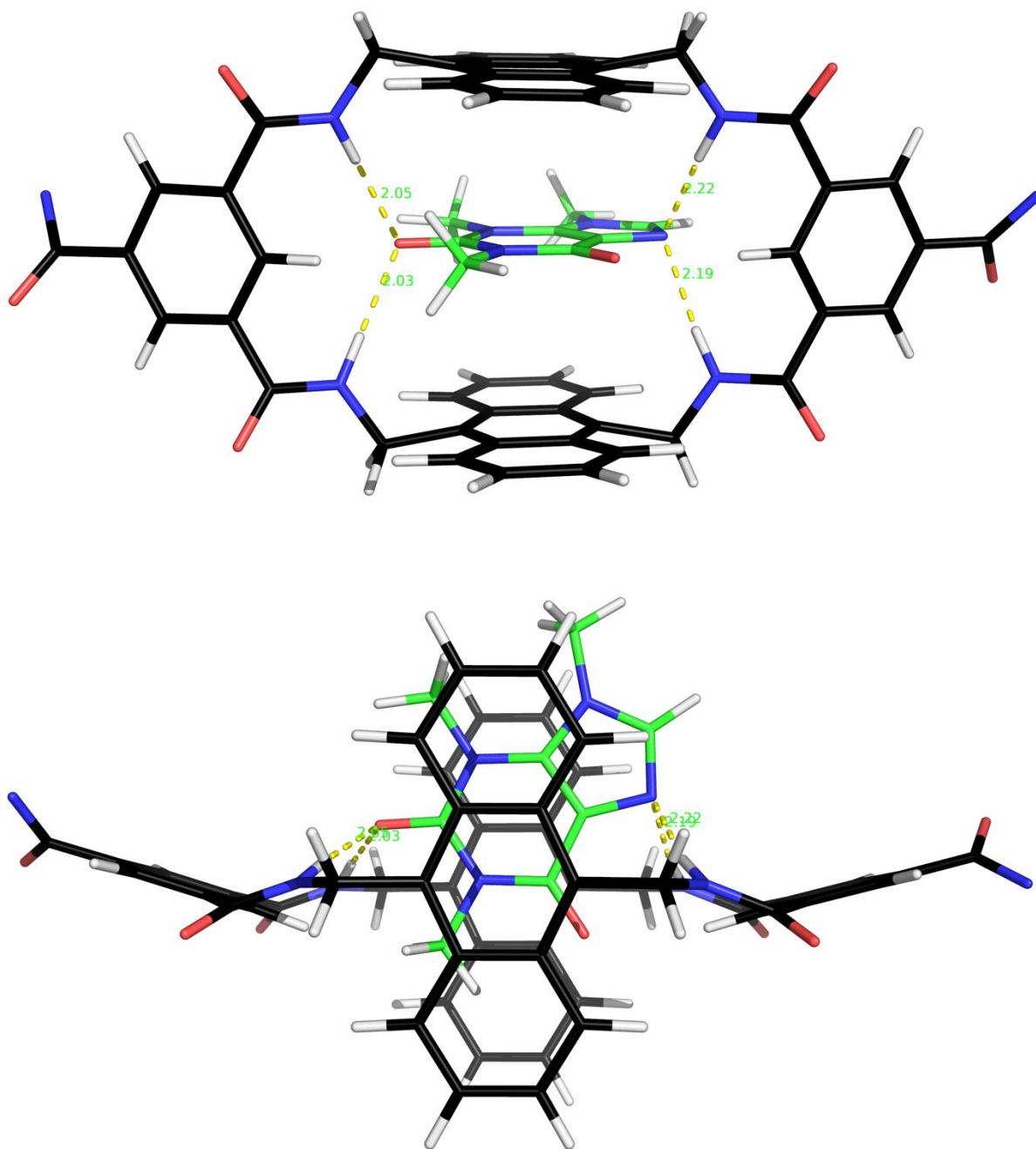


Figure S36. Model of caffeine **4** bound to receptor **1**, shown from two perspectives. Intermolecular hydrogen bonds are shown as yellow dashed lines. Side-chains are omitted for clarity.

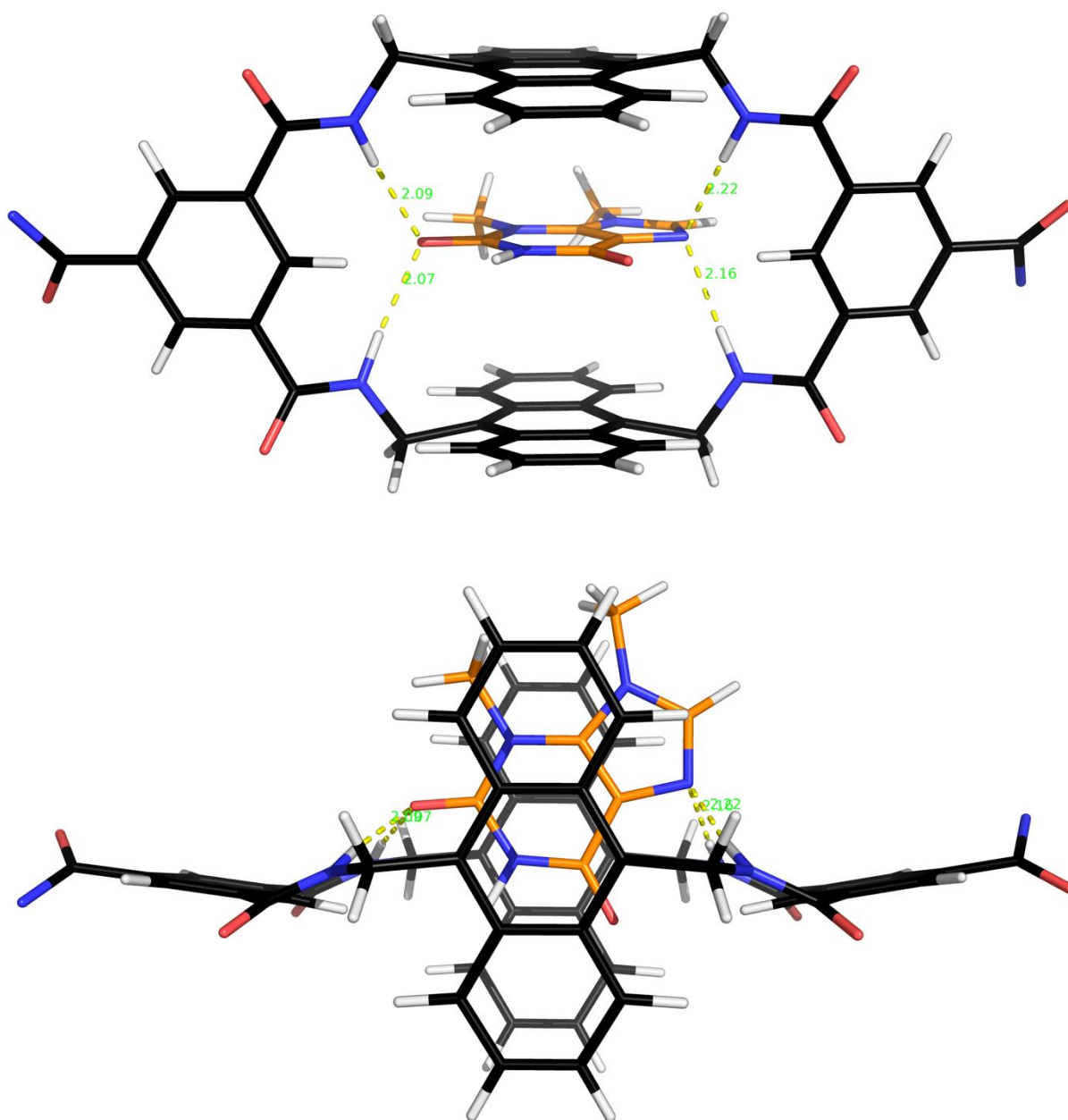


Figure S37. Model of theobromine **5** bound to receptor **1**, shown from two perspectives. Intermolecular hydrogen bonds are shown as yellow dashed lines. Side-chains are omitted for clarity.

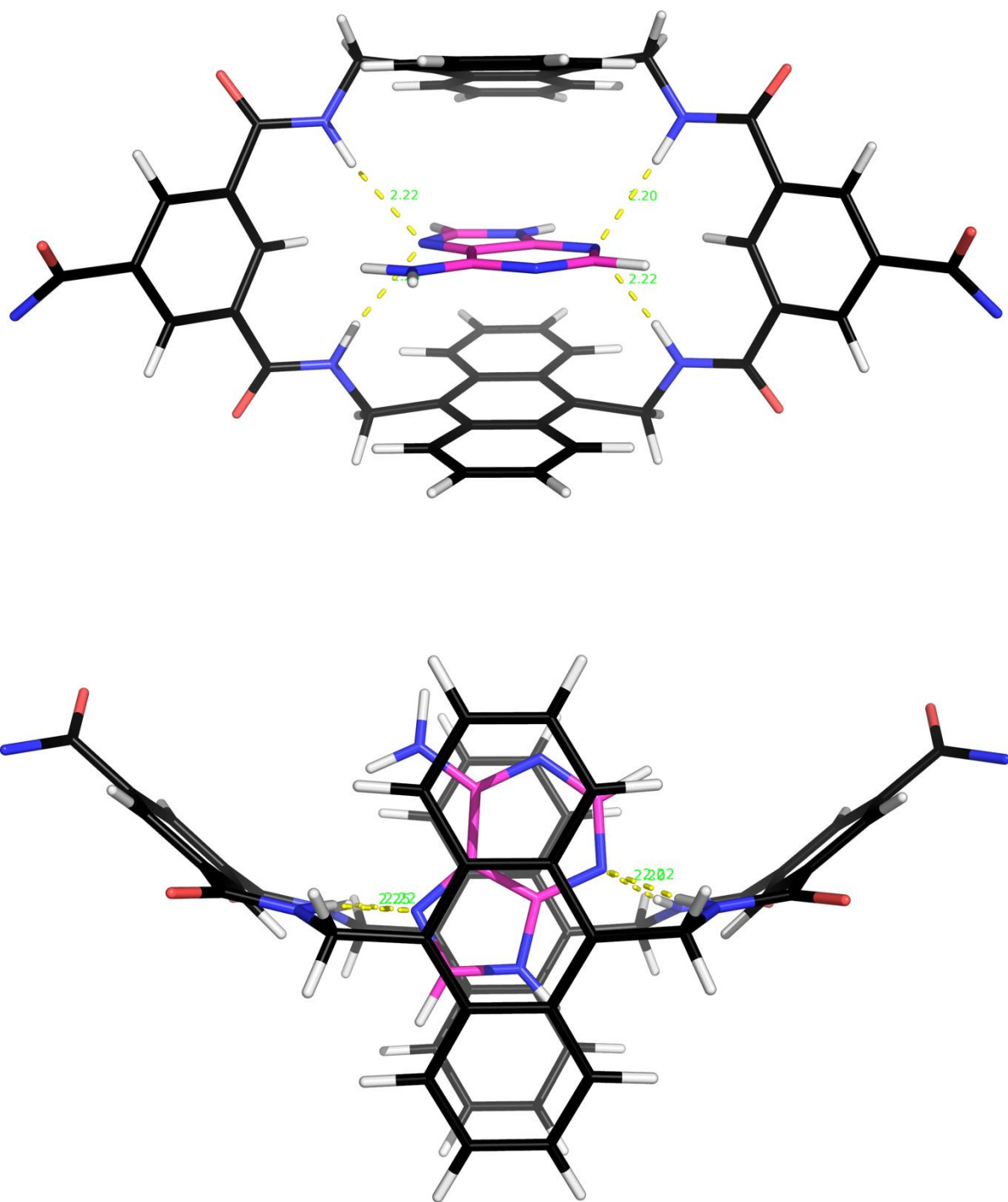


Figure S38. Model of adenine **6** bound to receptor **1**, shown from two perspectives. Intermolecular hydrogen bonds are shown as yellow dashed lines. Side-chains are omitted for clarity.

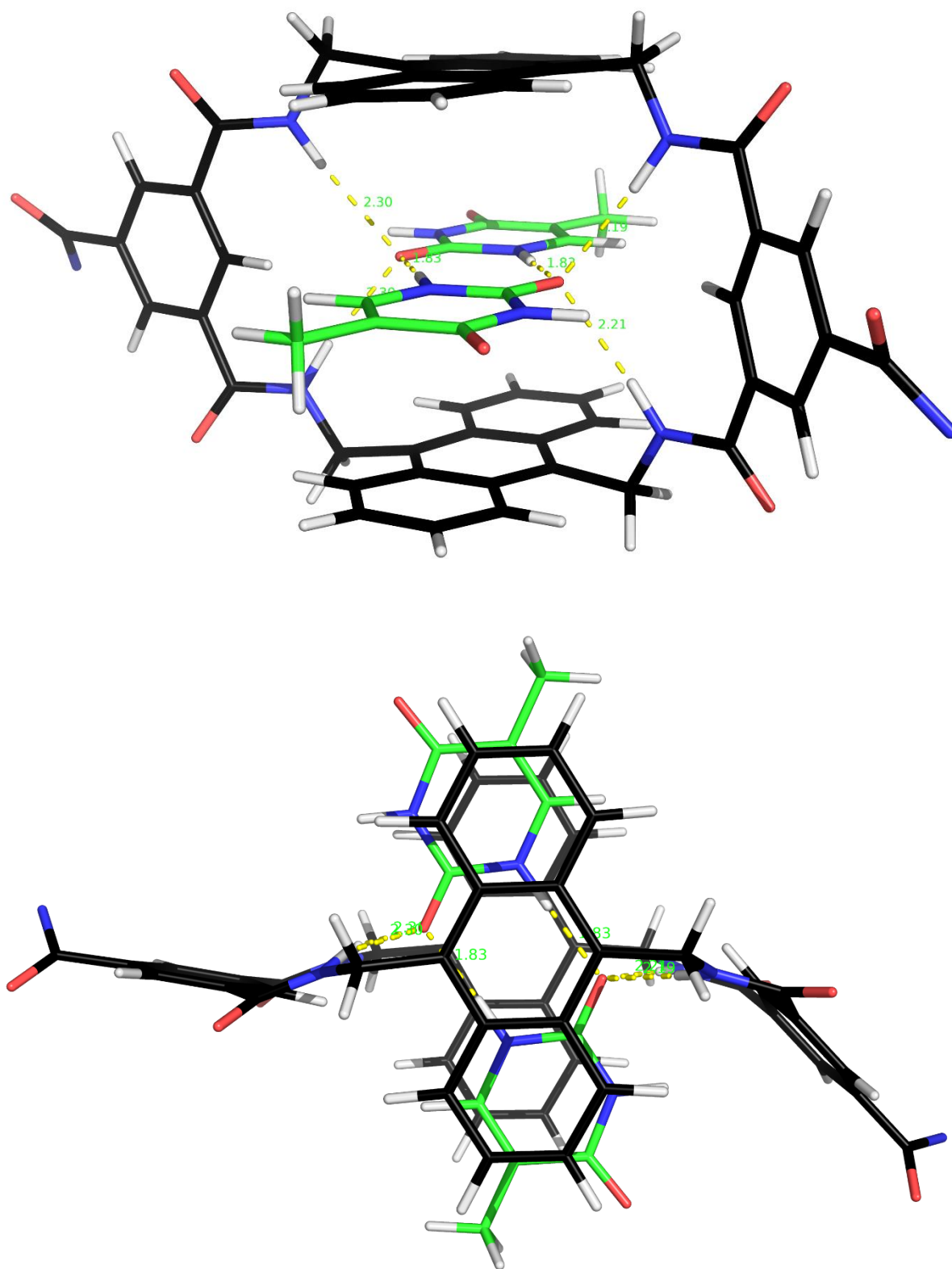


Figure S39. Model of $2 \times$ thymine **7** bound to receptor **1**, shown from two perspectives. Intermolecular hydrogen bonds are shown as yellow dashed lines. Side-chains are omitted for clarity.

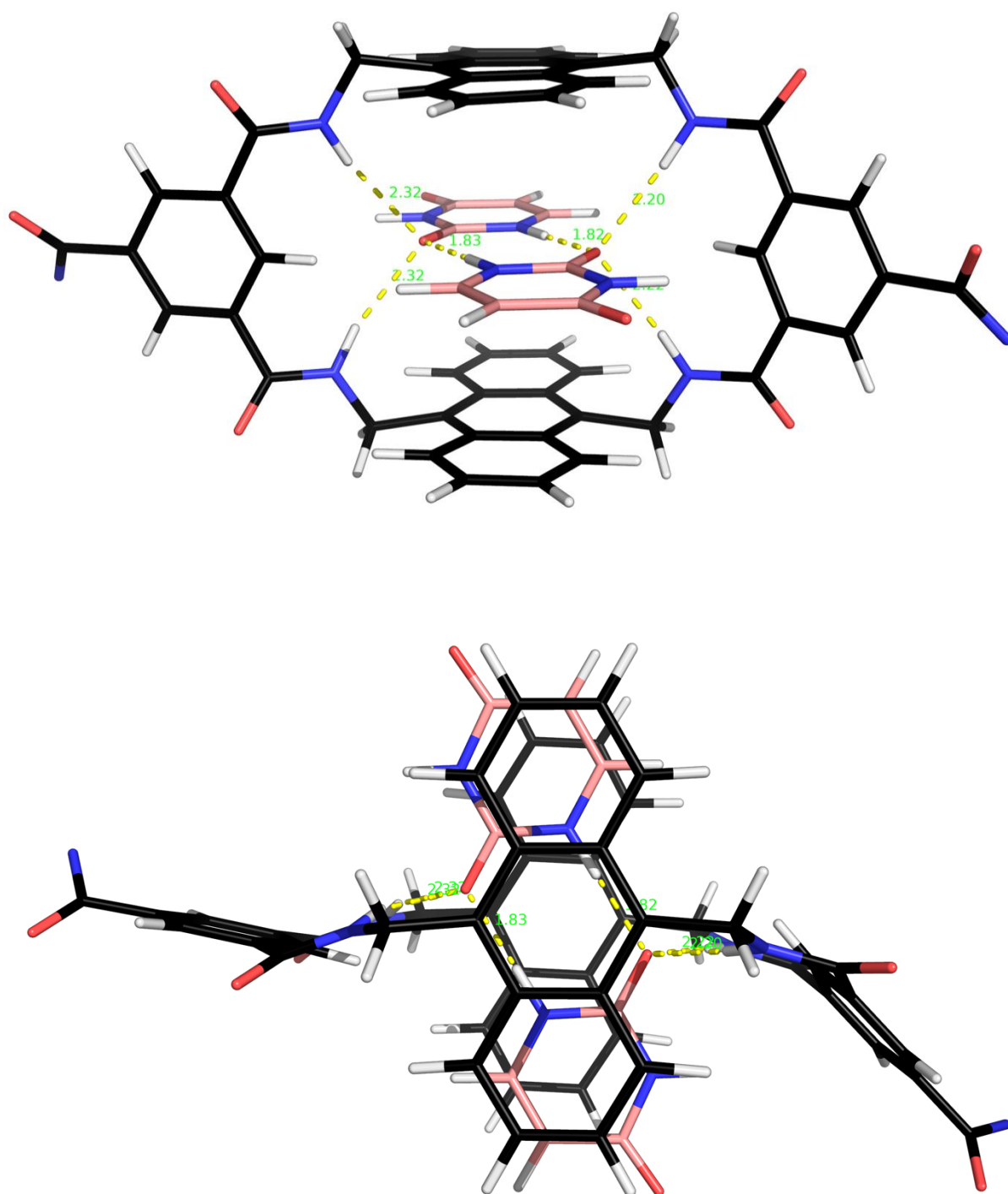


Figure S40. Model of $2 \times$ uracil **8** bound to receptor **1**, shown from two perspectives. Intermolecular hydrogen bonds are shown as yellow dashed lines. Side-chains are omitted for clarity.

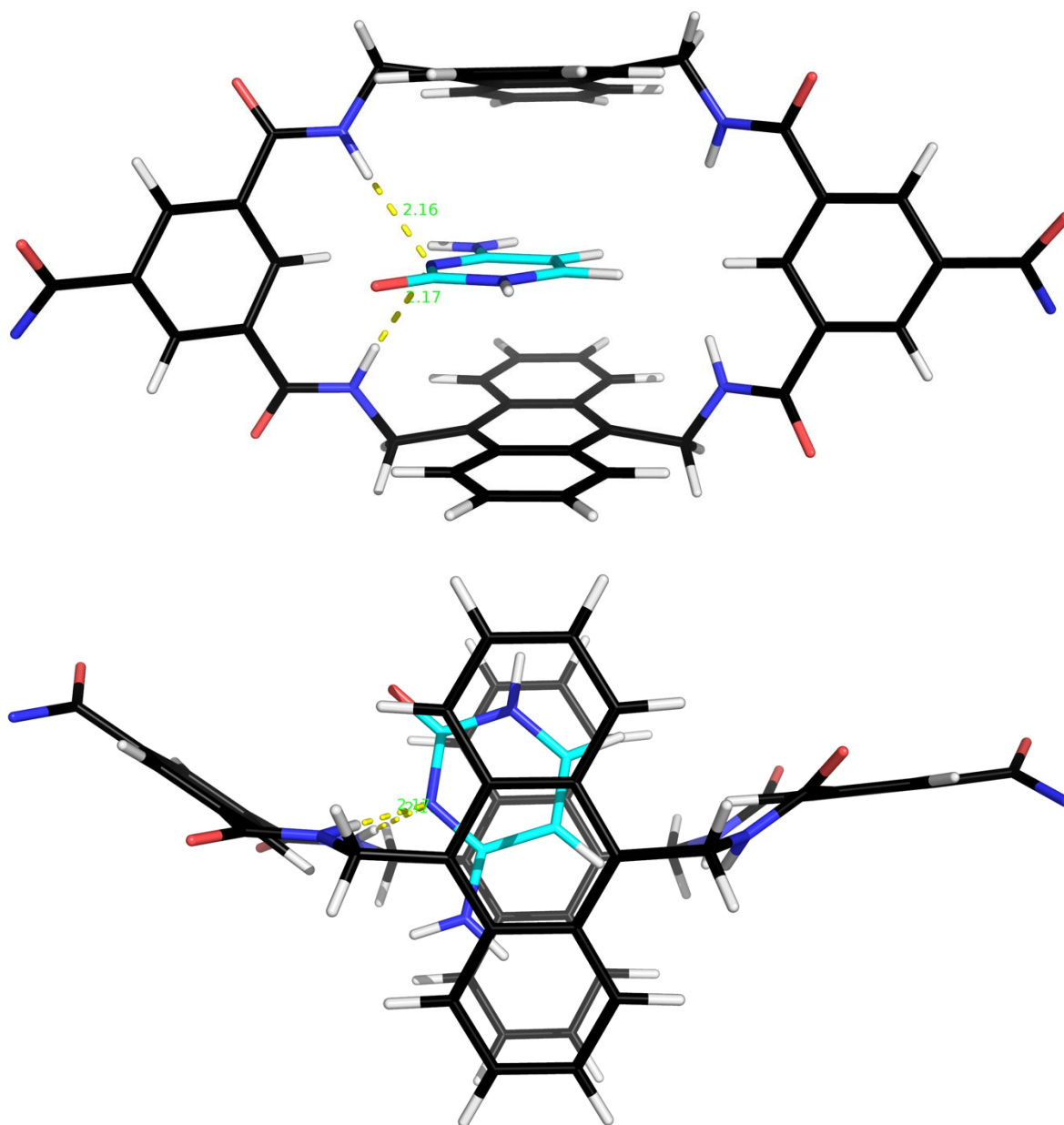


Figure S41. Model of cytosine **9** bound to receptor **1**, shown from two perspectives. Intermolecular hydrogen bonds are shown as yellow dashed lines. Side-chains are omitted for clarity.

References

1. H. Destecroix, C. M. Renney, T. J. Mooibroek, T. S. Carter, P. F. N. Stewart, M. P. Crump and A. P. Davis, *Angew. Chem., Int. Ed.*, 2015, **54**, 2057-2061.
2. Bindfit 0.5, <http://app.supramolecular.org/bindfit/>, November 2019.
3. D. B. Hibbert and P. Thordarson, *Chem. Commun.* 2016, **52**, 12792-12805.